

---

## Modelling abrupt glacial North Atlantic freshening: Rates of change and their implications for Heinrich events

Bigg Grant R. <sup>1,\*</sup>, Levine Richard C. <sup>1</sup>, Green Clare L. <sup>1</sup>

<sup>1</sup> Univ Sheffield, Dept Geog, Sheffield S10 2TN, S Yorkshire, England.

\* Corresponding author : Grant R. Bigg, email address : [grant.bigg@sheffield.ac.uk](mailto:grant.bigg@sheffield.ac.uk)

[richard.levine@metoffice.gov.uk](mailto:richard.levine@metoffice.gov.uk) ; [ggp05cj@sheffield.ac.uk](mailto:ggp05cj@sheffield.ac.uk)

---

### Abstract :

The abrupt delivery of large amounts of freshwater to the North Atlantic in the form of water or icebergs has been thought to lead to significant climate change, including abrupt slowing of the Atlantic Ocean meridional overturning circulation. In this paper we examine intermediate complexity coupled modelling evidence to estimate the rates of change, and recovery, in oceanic climate that would be expected for such events occurring during glacial times from likely sources around the North Atlantic and Arctic periphery. We show that rates of climate change are slower for events with a European or Arctic origin. Palaeoceanographic data are presented to consider, through the model results, the origin and likely strength of major ice-rafting, or Heinrich, events during the last glacial period. We suggest that Heinrich events H1-H3 are likely to have had a significant contribution from an Arctic source as well as Hudson Strait, leading to the observed climate change. In the case of H1 and H2, we hypothesise that this secondary input is from a Laurentide Arctic source, but the dominant iceberg release for H3 is hypothesised to derive from the northern Fennoscandian Ice Sheet, rather than Hudson Strait. Earlier Heinrich events are suggested to be predominantly Hudson Strait in origin, with H6 having the lowest climate impact, and hence iceberg flux, but H4 having a climate signal of geographically variable length. We hypothesise that this is linked to a combination of climate-affecting events occurring around the globe at this time, and not just of Laurentide origin.

**Keywords** : Heinrich events, modelling, Quaternary, icebergs

## 34 **1. Introduction**

35 The sedimentary record in the glacial (Marine Isotope Stage 2-3) North Atlantic domain is  
36 rich in complexity. Marine, ice and terrestrial records show evidence for long term climate  
37 decline interspersed by periods of more pronounced temperature decline and sharp, but short-  
38 lived, temperature rises (Fig. 1). Marine records show clear evidence for a number of times of  
39 sedimentary fall-out from enhanced iceberg rafting in the North Atlantic – Heinrich events –  
40 during this period (Hemming, 2004). There is also evidence for catastrophic freshwater  
41 outbursts from under ice sheets or ice-dammed lakes (e.g. Fisher, 2003; Leverington and  
42 Teller, 2003; Lekens et al., 2006; Murton et al., 2010). The Younger Dryas (YD) is the  
43 canonical event of this type, but while having a St. Lawrence origin, there is evidence that  
44 other, later contributions from the Arctic (Leverington and Teller, 2003) and Northern Europe  
45 (Nesje et al., 2004) may have prolonged the freshwater supply.

46 This tendency for abrupt change is centred in the Northern Hemisphere, and particularly  
47 the North Atlantic, having little signature in the Antarctic (Voelker, 2002). The classical  
48 portrayal of these signals is seen in the oxygen isotope, and hence temperature, record of the  
49 Greenland ice sheet, where the abrupt warmings became known as Dansgaard-Oeschger (D-  
50 O) events (Dansgaard et al., 1984). The linkages between these semi-periodic events and the  
51 ice-rafting peaks of Heinrich events became hypothesised as part of the Bond cycle (Bond et  
52 al., 1999), with a series of D-O events caused by stochastic freshwater forcing leading to ice  
53 accumulation on North American ice sheets that then became unstable and purged ice  
54 (Timmermann et al., 2003). These massive releases of icebergs are hypothesised to lead to  
55 major climate change and cessation of the Atlantic thermohaline circulation (Broecker,  
56 1994).

57 However, the origin of these abrupt climate changes is not well established, even though  
58 there is good evidence for their existence in various forms of palaeoclimatic archives. A  
59 recent review by Clement and Peterson (2008) surveyed the many records around the world,  
60 demonstrating the existence of the abrupt climate change during the last glacial period and  
61 discussed the three main mechanisms proposed for their cause: ocean thermohaline  
62 circulation change, sea-ice feedbacks and tropical processes. Their well argued conclusion  
63 was that none of these fitted the observations when compared with models of the different  
64 processes and that more work considering other, or combined, feedbacks using coupled  
65 climate models are required to understand abrupt change.

66 A subset of environmental change during the last glacial period consists of Heinrich  
67 events. These are periods, of  $500\pm 250$  years duration (Hemming, 2004) occurring roughly  
68 every 10 000 years, with extensive deposits of ice-rafted debris (IRD) in the North Atlantic  
69 marine record. These peaks of IRD are normally ascribed to episodic iceberg releases from  
70 the Hudson Strait Ice Stream of the Laurentide Ice Sheet, set off by binge-purge oscillations  
71 within the ice sheet (MacAyeal, 1993). There is good lithological evidence linking the IRD to  
72 North America (e.g. Grousset et al., 1993; Gwiazda et al., 1996a). However, there are other  
73 theories for their generation, and alternative possible sources, including the Fennoscandian  
74 Ice Sheet, particularly for Heinrich events H3 (~ 30 000 cal. yr B.P.) and H6 (~60 000 cal. yr  
75 B.P.) (Gwiazda et al., 1996b). These two events appear to be smaller in magnitude and may  
76 have multiple sources, or have an insufficiently large primary source to overwrite the lithic  
77 signature of more normal glacial IRD levels in the eastern Atlantic. It can sometimes be  
78 difficult to distinguish lithic signatures from the two sides of the North Atlantic (Farmer et  
79 al., 2003), however. Hemming (2004) gives an excellent review of the state of knowledge  
80 concerning Heinrich events, their causes, origins and the spread of IRD.

81 Whatever their origin, Heinrich events provide an unequivocal signal of disturbance to the  
82 marine environment through enhanced iceberg fluxes. There is also evidence of disturbance  
83 to the atmosphere on a hemispheric scale, through enhanced dust deposits from Asia in the  
84 Greenland ice cores (Biscaye et al., 1997), and, since Bond et al. (1993), a link has frequently  
85 been made between climate cooling, followed by abrupt warming, and Heinrich events. The  
86 classic picture is that the release of icebergs into the North Atlantic, and their subsequent  
87 melting, stabilises the surface ocean, preventing deep convection, and so shutting off the  
88 Atlantic meridional overturning circulation (Broecker, 1994). A wide range of climate  
89 modelling experiments have demonstrated that this scenario is consistent with climate  
90 physics (e.g. Rind et al., 2001; Ganopolski and Rahmstorf, 2001; Vellinga and Wood, 2002;  
91 Stouffer et al., 2006; Levine and Bigg, 2008; see Clement and Peterson (2008) for a full  
92 review).

93 In this paper we take an intermediate complexity climate model, spun-up for glacial  
94 climates and with iceberg-ocean coupling embedded within it (Levine and Bigg, 2008), to  
95 examine the rates of climate change in the glacial world consistent with a range of release  
96 rates of icebergs and freshwater into the North Atlantic and Arctic, from a range of possible  
97 source regions. The modelled rates of change are then compared with observed rates of  
98 change during the Younger Dryas and Heinrich events H1-H6 in a range of climate-related

99 indices. This allows us to comment on the origin and magnitude of these unequivocal abrupt  
100 freshwater events, and their true, individual, climate impact.

101 We first discuss the climate model and the range of experiments used to simulate  
102 freshwater or Heinrich event-led change to the Atlantic overturning. The results of the  
103 modelling experiments are then discussed. We next present the high temporal resolution  
104 glacial ocean, terrestrial and cryosphere proxy climate indices, followed by a comparison of  
105 the modelled rates of change with rates of change found in these climate indices around the  
106 time of Heinrich events. We conclude by discussing the implications of these comparisons for  
107 the strengths and origins of the Younger Dryas and H1-H6, and the consequences for our  
108 understanding of abrupt change during glacial times.

109

## 110 **2. Model**

111 The climate model used is an intermediate complexity coupled ocean-atmosphere model,  
112 with an energy balance atmosphere derived from that of Fanning and Weaver (1996) and a  
113 curvilinear coordinate ocean model, whose North Pole has been displaced to central  
114 Greenland (Wadley and Bigg, 1999). There is a free surface to the ocean (Webb, 1996) and a  
115 dynamic and thermodynamic sea-ice model at the interface of the ocean and atmosphere  
116 (Wadley and Bigg, 2002). In addition, icebergs are allowed to move, and melt, within the  
117 model in a way that is coupled to the ocean model processes (Levine and Bigg, 2008). The  
118 model's curvilinear grid enhances model resolution in the North Atlantic and Arctic, and in  
119 particular in the Greenland and Labrador Seas. Typically, in the Nordic Seas the horizontal  
120 resolution is  $1\text{--}2^\circ$ , whereas in the Southern Hemisphere it is  $6\text{--}8^\circ$ . Time step length is a  
121 function of grid spacing, to allow efficient integration of the variable resolution grid (Wadley  
122 and Bigg, 1999). Full details of the model can be found in Levine and Bigg (2008).

123 Here we are interested in abrupt change during glacial times, so the model experiments all  
124 start from a glacial control state. This state, and the equivalent representation of the climate  
125 for a present day control, is described in Levine and Bigg (2008). The background iceberg  
126 flux for the glacial Northern Hemisphere uses that calculated by Bigg and Wadley (2001),  
127 based on a steepest gradient algorithm draining atmospheric precipitation fields, from the  
128 atmospheric general circulation model runs for the Last Glacial Maximum (LGM) by Dong  
129 and Valdes (1998), off the Peltier (1994) ice sheet in a state of mass balance. For the  
130 Southern Hemisphere we use climatological iceberg fluxes from Gladstone et al. (2001) that  
131 are based on Present Day mass balance calculations for the Antarctic ice sheet. The Antarctic

132 ice sheet has decreased in volume since the LGM, however, there is evidence from cores  
133 taken at various latitudes in the South Atlantic that IRD delivery was at a minimum at periods  
134 surrounding the LGM and during the Holocene (e.g., Kanfoush et al. (2000)). We assume the  
135 Antarctic ice sheet to be in a steady state for both PD and LGM simulations and thus use the  
136 PD iceberg fluxes for both PD and LGM simulations.

137

### 138 *2.1. Control Run*

139 The performance of the PD model provides guidance for interpreting the reliability of the  
140 glacial simulations. Thus, the PD coupled model (see Levine and Bigg, 2008) has a rather  
141 high peak North Atlantic overturning of  $28.1 \pm 0.3$  Sv although the amount of North Atlantic  
142 Deep Water (NADW) that flows southward across the equator contributing to the global  
143 thermohaline circulation is only  $\sim 13$  Sv, which is reasonably consistent with observations  
144 (Gordon, 1986; Schmitz, 1995). The PD sea surface properties compare reasonably well with  
145 the climatological values, although gradients are not fully resolved. This is particularly true  
146 for the modelled meridional temperature gradients across the Southern Ocean, because of the  
147 relatively coarse resolution of the grid in this region, leading to a weak Antarctic Circumpolar  
148 Current ( $63.5 \pm 4.2$  Sv) compared to observations (130-140 Sv, Nowlin and Klinck (1986)).  
149 However, the temperature and salinity distribution in the northern North Atlantic and Nordic  
150 Seas corresponds quite well with the climatology and leads to realistic North Atlantic Deep  
151 Water formation, in terms of convection location and depth penetration. The tropical sea  
152 surface temperature (SST) and air temperature are a little low, leading to reduced evaporation  
153 and fresher tropical sea surface conditions than observed, with salinity anomalies over 1 psu.  
154 There is also less sea-ice in both hemispheres. In the Northern Hemisphere this anomaly is  
155 mainly on the continental shelves of the Arctic Ocean, and so does not directly influence the  
156 Atlantic convection areas. The Southern Hemisphere sea-ice areas of  $1.7 \pm 0.1$  million km<sup>2</sup>  
157 compares with observations of around 11 million km<sup>2</sup> for the annual mean (Cavalieri et al.,  
158 1997). However, poor reproduction of PD Southern Ocean sea-ice is a common climate  
159 model problem (Hansen et al., 2007).

160 The strength of northern Atlantic currents is an important factor in the speed with which  
161 salinity anomalies are moved around in the ocean, so it is relevant to examine the PD  
162 simulation's performance here. The strength of the North Atlantic sub-polar gyre ( $20.5 \pm 0.2$   
163 Sv) compares reasonably with the range in the literature (13-16 Sv according to Tomczak and  
164 Godfrey (2003)). The Denmark Strait Overflow in the model is 5-6 Sv, while observations

165 suggest it varies between 3-4 Sv (Macrander et al., 2005). Through the other route into the  
166 Nordic Seas the Faroe Shetland Channel has ~ 9 Sv of Atlantic inflow in the model, but  
167 observations suggest ~ 7 Sv (Østerhus et al., 2005). The model therefore produces  
168 reasonable, but slightly too large, fluxes into and out of the Arctic.

169  
170 In the glacial control run the main North Atlantic convection occurs to intermediate  
171 depths, with a maximum penetration to 1800 m. This is centred at 45°N in the central and  
172 eastern Atlantic, which is consistent with other studies suggesting the shallower convection  
173 of the last glacial period occurred south of Iceland (Seidov and Maslin, 1999). The strength  
174 of this is only a third ( $9.6 \pm 0.3$  Sv) of the PD peak overturning. This is within the uncertainty  
175 ranges provided by palaeo-observations (see Levine and Bigg (2008) for a fuller discussion).  
176 Estimates of coupled models of the LGM vary widely for this quantity (Weber et al., 2007),  
177 and the present model falls within this range of model uncertainty. Our modelled sea surface  
178 temperatures in the tropics and subtropics are lower than CLIMAP, which is consistent with  
179 the MARGO glacial analysis (Kucera et al., 2005). However, the winter limits of near  
180 freezing ocean surface temperatures in the model between 40–50°N are further south than in  
181 the MARGO reconstructions. Thus, our model produces sea-ice all year round in the Nordic  
182 Seas, while this area is thought to have been seasonally ice-free (Pflaumann et al., 2003;  
183 Kucera et al., 2005). This problem is similar to the experience of other LGM coupled models  
184 (Kageyama et al., 2006). In the SH the Drake Passage flux ( $88.6 \pm 2.3$  Sv) is a third higher  
185 than for the PD simulation. There is a five-fold increase in SH sea-ice area, to  $9.3 \pm 0.9$  million  
186 km<sup>2</sup>. This amount of Southern Ocean sea-ice is still approximately 20% lower than the PD  
187 observed annual mean but covering a much more realistic extent of ocean.

188

## 189 *2.2. Experiments*

190 In this paper we are examining the signature of abrupt change resulting from known  
191 catastrophic adjustments to last glacial ice sheets, either through fresh water release (e.g. the  
192 Younger Dryas) or iceberg melting (the Heinrich events). Consequently, we performed a  
193 number of experiments where the basic glacial control run of the model was perturbed by  
194 freshwater or iceberg additions from a number of possible release locations around the North  
195 Atlantic and Arctic periphery (Fig. 2). The length of time during which the perturbation was  
196 imposed was determined from estimates in the literature. The extensive review of Heinrich  
197 events in the palaeoceanographic literature by Hemming (2004) suggested a period of 500

198 ±250 years. We have therefore imposed our perturbations for 500 years, after 5500 years of a  
199 glacial control simulation, and run on the experiments for at least an additional 500 years to  
200 study the rate of return of the climate towards an unperturbed state. Green (2009) showed that  
201 while changing the duration of the pulse affects the detail of the response, the general  
202 character is the same. We have examined a range of possible freshwater-equivalent release  
203 rates, ranging over 0.1-0.4 Sv. These match with estimates from the palaeoceanographic  
204 (Hemming, 2004; Roche et al., 2004) and modelling (Calov et al., 2002) communities; they  
205 also cover a range over which our model response varies from a circulation perturbation to a  
206 complete collapse (Levine and Bigg, 2008).

207 The release locations have been chosen through field evidence of known or suspected  
208 catastrophic events. The ice stream feeding Hudson Strait has long been acknowledged as a  
209 likely source for Heinrich events (Broecker et al., 1992) because of the lithology of North  
210 Atlantic IRD, the latter's strong carbonate content, which is characteristic of sediments  
211 underlying Hudson Bay, and the geographic pattern of IRD deposition. The ice stream  
212 draining through the Gulf of St. Lawrence overlay areas of similar geology to the Hudson  
213 Strait ice stream, and would have produced icebergs feeding into the same North Atlantic  
214 IRD pattern. There is evidence that IRD in Heinrich deposits has a signature consistent with  
215 at least a contribution from the Gulf of St. Lawrence (Piper and Skene, 1998; Piper and  
216 DeWolfe, 2003). We have therefore used this as a second release location. Further afield,  
217 there has been debate over a European origin for H3 and H6. While this now seems less  
218 likely (see Hemming (2004) for a review) there is increasing evidence for an ice-bridge  
219 across the northern North Sea (Sejrup et al., 2009) and a major ice stream in the Norwegian  
220 Channel (Nygård et al., 2007), either of which are possible candidates for major ice release  
221 from the southern arm of the Fennoscandian Ice Sheet, at least for H3 (Lekens et al., 2009).

222 The Arctic also provides potential release sites for either iceberg or freshwater releases.  
223 Iceberg scour marks and erosion on the deep Lomonosov Ridge in the central Arctic and the  
224 Yermak Plateau northwest of Svalbard are consistent with a catastrophic release of deep draft  
225 icebergs from the northern Barents Sea section of the Fennoscandian ice sheet (Kristoffersen  
226 et al., 2004; Green et al., 2010). There is evidence that the very deep St. Anna Trough in the  
227 eastern Barents Sea continental margin had ice grounded to its base during the last glacial  
228 period (Polyak et al., 1997). This, or the nearby Franz Victoria Trough (Green et al., 2010),  
229 therefore represents a possible source for a catastrophic release of icebergs. Finally, the  
230 Mackenzie basin and M'Clure Strait in western Arctic Canada drained the Keewatin Dome of

231 the Laurentide Ice Sheet. The Mackenzie is likely to have been the route down which there  
232 was a freshwater release during the Younger Dryas, through a partial collapse of Lake  
233 Agassiz (Teller et al., 2002, Murton et al., 2010). There were also major ice-rafting events  
234 during the Last Glacial from the M'Clure Strait in the western Canadian Archipelago (Stokes  
235 et al, 2005; Darby and Zimmerman, 2008). This therefore forms the fifth source region for  
236 our iceberg and freshwater release experiments (Fig. 2).

237

### 238 **3. Modelling Results**

239 In the modelling results presented below there is an intrinsic assumption that sufficient ice  
240 was present in the catchment of each release site during the Last Glacial for our range of  
241 fluxes to be possible. This may, or may not, be true for any particular time during this long  
242 time period but allows comparison of the impact between different release sites. Later  
243 sections will address the probability of such releases within the palaeoclimate data  
244 assessment.

#### 245 *3.1. Iceberg experiments*

246 The clearest variable to show the response of the climate to the iceberg forcing is the  
247 strength of the peak Meridional Overturning Circulation (MOC) of the North Atlantic. This is  
248 shown for the 1000 years following the start of release of icebergs at fluxes of 0.1 Sv, 0.2 Sv  
249 and 0.4 Sv from the five release points around the North Atlantic and Arctic in Fig. 3. The  
250 control run's MOC is also shown for comparison.

251 In all cases the 0.1 Sv release causes a decline in the strength of the MOC by 2-3 Sv, or  
252 20%, with an eventual recovery of some extent. However, the speed of the decline, and the  
253 recovery, depend on the location of the iceberg release. The majority of the decline occurs  
254 within a decade from eastern North American releases, while from other locations it is  
255 slower, up to 1-200 years. There is also a difference in the rate of recovery once the iceberg  
256 release ceases in Year 6000 of the model run. The eastern North American release  
257 experiments show a rapid return of the MOC to values near those of the control. However,  
258 the recovery of eastern Atlantic and Arctic release experiments is significantly more gradual,  
259 taking at least a century, but up to 300 years from Mackenzie releases. In the case of the St.  
260 Lawrence release, the MOC does not recover to its original level but equilibrates at a new,  
261 slightly lower, MOC strength.

262 This tendency to equilibrate at a new MOC level on recovery is seen in several of the  
263 experiments with higher releases (Fig. 3). This new equilibrium state after recovery is not



264 invariably one with a lower MOC, and hence colder North Atlantic, but can lead to a higher  
265 MOC (for example, the 0.2 Sv St. Anna Trough release). The equilibrium recovery behaviour  
266 is very dependent on the specific release location, but the rates of change respond to a  
267 broader geographical imperative. Thus, rates of initial decline are always very rapid from  
268 eastern North American releases whatever the release strength, while the behaviour of  
269 experiments from other release sites varies with the release magnitude. For these sites the 0.2  
270 Sv and 0.1 Sv releases result in similar behaviour, however, the rate of decline is faster when  
271 collapse of the MOC occurs for 0.4 Sv releases, if still up to a few decades slower than for  
272 collapse generated from eastern North America.

273 Recovery rates are generally independent of the release magnitude, but dependent on the  
274 release site. Thus, for eastern North American release experiments recovery is extremely  
275 rapid, Mackenzie experiments recover over about a century, while NCIS and St. Anna  
276 Trough release experiments require several hundred years for recovery. Note that for the  
277 stronger releases only Hudson Strait and Mackenzie experiments show consistent recovery to  
278 pre-release MOC strengths.

279 The explanation for the sometimes striking differences between the oceanic responses to  
280 release location lies in where the fresh water from the iceberg melting enters the ocean and  
281 the consequent response of the ocean density field, currents and ocean and atmospheric  
282 temperature fields. The icebergs are released in a range of sizes (Levine and Bigg, 2008) and  
283 allowed to move, and melt, through the interaction of the icebergs with the ocean and  
284 atmosphere (Bigg et al., 1997). The bergs will melt rather slowly in cold conditions, and  
285 those originating in the Arctic may take some years to decades (Bigg et al., 1996; Green,  
286 2009) to leave this Ocean. Rapid melting, and so addition of freshwater to the ocean, only  
287 occurs once the icebergs enter warmer and windier climates (Bigg et al., 1997). Note that this  
288 may not relate closely to where IRD is deposited (Death et al., 2006).

289 Due to all these factors, the model salinity fields reveal the path along which icebergs  
290 travel, and melt, once they are released, rather than the result of freshwater advection and  
291 diffusion from a point source. The sea surface salinity fields for the control and 0.4 Sv  
292 experiments are shown in Fig. 4 300 years after the catastrophic iceberg releases began. The  
293 release points on the eastern coast of North America show the movement of icebergs into the  
294 glacial Gulf Stream and North Atlantic Drift with freshwater entering this system and then  
295 moving south into the sub-tropical gyre re-circulation. Rather little impact is seen in the sub-  
296 polar gyre and Arctic, as few icebergs from these sources penetrate into such regions, and

297 relatively little surface water advects unaltered from the modelled glacial sub-tropical gyre  
298 northwards. The freshwater does, however, enter the region of intermediate water formation  
299 in the central North Atlantic rather quickly, hence leading to rapid decline of the MOC, and  
300 almost as rapid a return once this source is cut-off and the fresh anomaly of the NW Atlantic  
301 has been advected past the convection region.

302 In the case of a Mackenzie release, Fig. 4 shows that much of the freshwater, as both ice  
303 and freshwater, leaves the Arctic in the East Greenland Current and then freshens the  
304 Labrador Sea and northwestern Atlantic. The Arctic is also freshened generally. Thus there is  
305 a delay in the MOC decline, as shown by Fig. 3, relative to eastern North American releases,  
306 as it takes longer for sufficient freshwater to enter the northern Atlantic, both from the delay  
307 due to the water transit time and the slow melting of icebergs in a cold Arctic and Greenland  
308 Sea. The cessation of iceberg input also leads to a slower recovery because it takes some  
309 decades to centuries, depending on the run, for the excess salinity built-up in the Arctic to be  
310 flushed out into the ocean more generally.

311 The European releases show this delay in the onset of MOC decline (Fig. 3), but respond  
312 rather differently to North American releases thereafter. Many of the NCIS icebergs go north  
313 and melt in the Nordic Seas, or Arctic, while relatively few of the St. Anna Trough icebergs  
314 get entrained into the East Greenland Current and exit into the NW Atlantic. In both cases,  
315 this leads to large-scale freshening in the Northeastern Atlantic and eastern Arctic, which  
316 creates a pool of low salinity that gradually leaks out into the Atlantic, and results in a  
317 continuation in MOC decline beyond the time of initial response, unless the circulation was  
318 shut down (Fig. 3). Similarly, once the iceberg input ceases this slow leaking of freshwater  
319 significantly delays the return to a strong MOC. It must be remembered that there is a net  
320 decrease in global salinity due to the Heinrich events, but while North American inputs tend  
321 to get mixed globally to minimise the net impact of this on the MOC, the eastern Arctic input  
322 leads to a long-term decrease of the North Atlantic salinity field. In this case, areas between  
323 ~50-60°N retain upper ocean salinity values some 1 ‰ lower even 500 years after the iceberg  
324 input has ceased.

325 The SST patterns tend to be similar for the different events because they are strongly tied  
326 to the strength of the MOC. Thus, there is significant cooling over the central Atlantic, as the  
327 North Atlantic Drift adjusts southwards, and some weak warming further north and south  
328 (Levine and Bigg, 2008). This is similar to the results of Vellinga and Wood (2002) for a  
329 present day freshwater release. For atmospheric temperature anomalies, again there is cooling

330 over the North Atlantic, whose centre and magnitude varies depending on the release site (see  
331 Levine and Bigg, 2008). The Mackenzie and NCIS releases produce the maximum cooling,  
332 and so biggest overall climatic effect. Note that all releases lead to some, at least localised,  
333 warming; for the Hudson Strait release circum-Arctic warming is a strong characteristic, with  
334 the maximum warming centred over northern Greenland (Fig. 5). Releases from the St. Anna  
335 Trough also lead to localised warming over northeastern Greenland, and slight warming over  
336 the eastern Arctic and much of northern Eurasia. Releases from the St. Lawrence, NCIS and  
337 to a lesser extent, the Mackenzie, result in significant western European cooling.

338

### 339 *3.2. Freshwater experiments*

340 The MOC values for the freshwater release experiments are shown in Fig. 6. These are  
341 similar to the iceberg releases in character, both in terms of the relative rates of change and  
342 the recovery. In the case of releases from eastern North America, the main difference is that  
343 the MOC reacts more to weaker inflows, but the rates are very similar as the fresh water is  
344 effectively injected into the same current systems in both iceberg and freshwater releases. In  
345 contrast, the Mackenzie release has less impact per unit freshwater equivalent release because  
346 the freshwater enters the western Arctic directly, rather than being carried further towards the  
347 North Atlantic as icebergs before release. More of the freshwater therefore remains in the  
348 Arctic for longer, reducing the impact, although also slowing the recovery somewhat.

349 Freshwater releases from the European sites show substantially larger impacts on the  
350 MOC than do similar iceberg releases. The freshwater in both cases reaches the central North  
351 Atlantic convection zone in a few decades and caps the ocean. In fact, the releases from both  
352 the NCIS and St. Anna Trough cause such rapid change that the model becomes numerically  
353 unstable for larger releases.

354

### 355 *3.3. Experimental summary*

356 Several key differences between sites of release and the type of freshwater release are  
357 apparent from these numerical experiments. Firstly, whatever form the release takes, inputs  
358 from eastern North America cause substantial and rapid change in North Atlantic climate,  
359 with equally rapid recovery to states similar to the original climate. Secondly, Arctic and  
360 European releases of icebergs show a slower response of several decades to centuries for  
361 climate cooling, and similar, slower, timescales of recovery. Thirdly, experiments with

362 freshwater releases from these sites show a rapid onset of climate cooling but a slower  
363 recovery than is the case for experiments with eastern North American inputs.

364 The extent of the climate effect also depends on the release location and type. Iceberg  
365 inputs show a more linear variation with MOC decline, whatever the release site, until  
366 effective collapse occurs, than is the case for freshwater releases. For the latter, the MOC is  
367 most sensitive to releases from eastern North America (although the numerical problems  
368 caused by rates of change may distort this result).

369 We have here considered idealised experiments for a particular time, and hence orbital  
370 parameter, atmospheric carbon dioxide concentration and ice sheet configuration. We have  
371 also considered single release experiments, rather than the impact of multiple release sites on  
372 glacial ocean circulation and climate, in order to disentangle the basic signature deriving from  
373 each release site. It is possible, indeed likely, that any observed palaeoclimatic signal will not  
374 have been due to such a pure event as we have modelled. Nevertheless, sensitivity  
375 experiments that we have performed using different glacial forcings and combinations of  
376 releases suggest that there is sufficient signal produced in the idealised experiments for us to  
377 usefully proceed to explore the palaeoclimatic record. For example, mixing equal strength  
378 Arctic and Hudson Strait releases produces a response dominated by the Hudson Strait  
379 release, as the latter affects the convection site first, because of its proximity.

380 These idealised modelled differences therefore mean that it should be possible to attempt  
381 to infer rates, types and locations of releases from the rates, and absolute magnitudes, of  
382 change in the palaeoclimate record. In the following section we will examine such records  
383 with high temporal resolution, concentrating on the known freshwater release of the Younger  
384 Dryas (c. 11-12 000 cal. yr B.P.) and the known iceberg releases of Heinrich events H1-H6  
385 during the Weichselian.

386

## 387 **4. Palaeoclimate Analysis**

388

### 389 *4.1. Representative data sets*

390 To compare the numerical experimental conclusions with palaeodata it is necessary to  
391 look at a representative set of high resolution (sub-centennial) but long-term records covering  
392 the North Atlantic region where the climatic impact was seen to be strongest in the numerical  
393 experiments (Fig. 5). It has not been possible to find appropriate datasets to cover the whole  
394 of the period back to 70 000 cal. yr B. P. for all areas, but a representative sample of different

395 geographical regions and data types has been selected. Fig. 7 shows the location of the  
396 datasets chosen and Fig. 8 shows the various timeseries on a common timescale. These  
397 timeseries address different aspects of climate variability in regions where the model  
398 experiments showed most clearly defined differences between the different release  
399 experiments. No exactly comparable proxies with the necessary temporal resolution and  
400 scientific basis were discovered across the whole North Atlantic, where model difference was  
401 greatest. However, coverage is available in some manner in most crucial areas; we discuss  
402 drawbacks as well as advantages to using potentially problematic datasets in what follows.

403 Ice cores from Greenland provide an anchor against which many studies compare their  
404 local results; in addition Greenland is an area where we expect significant atmospheric  
405 climate change to be seen for the abrupt changes to be studied (Fig. 5). The GISP2 ice core  
406 record from central Greenland provides a temperature reconstruction from oxygen isotope  
407 and ice accumulation records extending back to 50 000 cal. yr B. P.. The original  
408 reconstruction derives from Cuffey and Clow (1997), with smoothing by Alley (2000).  
409 Another important indicator of change is the sea level record. A high resolution record of sea  
410 level should show the rate of transfer of freshwater, as either ice or water, from land to sea,  
411 and hence be a proxy for the temporal length and magnitude of an iceberg or freshwater  
412 release respectively. Siddall et al. (2003) used a combination of an oxygen isotope record  
413 from a Red Sea core with a hydraulic model of exchange between the Red Sea and the  
414 Arabian Sea to reconstruct sea level change, down to centennial scale for much of the last  
415 70,000 years.

416 The main indicator used for comparing the numerical experiments was the MOC strength  
417 (Figs. 3 and 6). There are few modern day records of this, let alone palaeo-records. However,  
418 one proxy is the sortable silt grain size of bottom sediments (McCave et al., 1995) under the  
419 deep return flow of the MOC in the North Atlantic. We use here such a timeseries, extending  
420 over 26-62 000 cal. yr B. P., that has been sampled at centennial to sub-centennial scale from  
421 ODP Site 1060 on the Blake Outer Ridge of the western Atlantic by Hoogakker et al. (2007).  
422 The mean grain size of the 10-63  $\mu\text{m}$  sediment fraction was used. Larger sizes imply stronger  
423 currents, and hence a stronger MOC. Previous work using this parameter, and a discussion of  
424 its advantages and drawbacks, can be found in McCave and Hall (2006).

425 The biggest climatic impact of abrupt North Atlantic freshwater injections is found in the  
426 North central Atlantic (e.g. Fig. 5). Hence SST indicators from either side of the Atlantic are  
427 also used. From the Gulf Stream dominated western region, a Marine Isotope Stage 3 record

428 (24 -64 000 cal. yr B. P.) of faunal and alkenone reconstructed SSTs is available (Vautravers  
429 et al., 2004) from the same site, ODP 1060, as is used for the MOC proxy. This will tell us  
430 about both the local atmospheric and upper ocean climate variability. In the eastern Atlantic,  
431 core MD01-2444 underlies a seasonally active upwelling zone off the Portuguese coast. The  
432 northern limit of this upwelling will move latitudinally as climate fluctuates, leading to SSTs  
433 from this site being a sensitive indicator of climate change. We use a faunal SST  
434 reconstruction covering a similar time period to that of the western Atlantic SST site to  
435 represent this area of North Atlantic climate (Vautravers and Shackleton, 2006). Another  
436 sensitive oceanic indicator of climate change is the exchange of water between the  
437 Mediterranean and the Atlantic through the Strait of Gibraltar, as this tells us something  
438 about the relative densities of the eastern Atlantic and Mediterranean, and therefore acts as a  
439 regional climate proxy (Rogerson et al., 2010) . We use a high resolution record of alkenone-  
440 derived SST in the Alboran Sea, at site MD952043, as an indicator of conditions near the  
441 exchange; this dataset is available back to 52 000 cal. yr B.P. (Cacho et al., 1999).

442 The numerical experiments indicate that the climate anomaly caused by some Heinrich  
443 events is likely to have spread over Europe (Fig. 5). Thus, from Lago Grande di Monticchio  
444 in southern Italy a high resolution 100 000 year record of carbon content in the lake  
445 sediments, measured through their loss fraction on ignition and the biogenic silica content  
446 (Allen et al., 1999) is used. These two indicators are linked to the proportion of the sediment  
447 entering the lake from erosion of bare or forested environments, thus high weight percentages  
448 for both are characteristic of high organic fractions in runoff, while low values suggest barer  
449 soils with rather low organic content. Both can approach zero in particularly cold climates.  
450 Such records may respond strongly to local topographic influences as much as the wider,  
451 regional climate. However, this particular record correlates strongly with changes in the  
452 Greenland ice core (Allen et al., 1999), suggesting that it is largely responding to large-scale,  
453 rather than local, influences.

454 A second terrestrial site is chosen from Brazil, as the numerical experiments suggest the  
455 cooling during Heinrich events caused by Hudson Strait releases may have led to a western  
456 Atlantic-centred cooling extending to South America, with potential impact on tropical  
457 climate teleconnections (Fig. 5). High resolution stalagmite oxygen isotope records,  
458 extending back to 116 000 cal. yr B. P., from the sub-tropical Botuverá Cave (Cruz et al.,  
459 2005) are used to examine climate change in this region. These data also act as an indicator of  
460 climate change in the Southern Hemisphere, to gauge the cross-equatorial spread of any

461 abrupt change. The oxygen isotope record appears to mostly be a reflection of the local  
462 precipitation record (Cruz et al., 2005), with less negative values reflecting more regional  
463 winter than summer rainfall because of a weakening of the strength of the local summer  
464 monsoon, which imports moisture from afar and is characterised by intense convection,  
465 during such times. Thus, the long-term signal is dominated by the precessional (21 000 year)  
466 orbital cycle. Nevertheless, over the short-term we can ignore this trend and examine  
467 evidence for abrupt change in the isotopic rate of change.

468

#### 469 *4.2. Evidence for abrupt change*

470 To examine our selected palaeoclimate records for abrupt change we first need to specify  
471 the time periods to examine. These are shown in Table 1. We follow Hemming (2004) for  
472 estimates of the timing of Heinrich events, and Alley (2000) for the Younger Dryas. The  
473 durations of these events are estimated as  $500\pm 250$  years (Hemming, 2004) for Heinrich  
474 events and 1500 years for the Younger Dryas, with a number of freshwater releases  
475 maintaining the oceanic freshening (Teller et al., 2002) in the case of the latter. In  
476 intercomparing records the question of the relative accuracy of their chronologies arises.  
477 Records with very well established calendar year chronologies have been chosen to minimise  
478 this problem, and in general, as we will see, there is very good agreement on the relative  
479 timings of events. However, here we are interested in rates of change in what are normally  
480 significant events. Thus, slight off-sets in the absolute time between the different records are  
481 not a major problem.

482 In the case of the Younger Dryas (YD) and Heinrich Event 1 (H1) a number of the chosen  
483 high resolution datasets do not cover this period so an additional high resolution, but shorter,  
484 SST dataset has been added from the Caribbean basin (Lea et al., 2003). Variations in these  
485 data are thought to indicate changes in the movement of the ITCZ (Lea et al., 2003), but they  
486 may also be linked to changes in the input of warm water to the sub-tropical gyre.

487 The palaeohydrological reconstructions of Leverington and Teller (2003) and Nesje et al.  
488 (2004) offer the current view of the YD being largely flood-induced, but with successive  
489 flooding from a range of locations prolonging the cooling event. Figure 9 shows a  
490 comparison of the various datasets through the YD. The Greenland temperature record shows  
491 very abrupt onset c. 12.9k cal. yr B.P. and abrupt recovery c. 11.6k cal. yr B.P.. These dates  
492 correspond quite well with change in the SST records across the Atlantic, particularly with an  
493 abrupt onset of cooler conditions. Recovery is also abrupt in the ice core record, but less so in

494 both SST records around the same time. The Brazilian ITCZ record also suggests a change to  
495 weaker ITCZ convection during the YD, indicating cooler conditions reaching into the  
496 Southern Hemisphere. The southern European terrestrial record shows little sign of the  
497 abrupt return to glacial conditions; the sharp spike around 12.2k cal. yr B.P. is seen in just  
498 one point and may be a data problem. The abrupt onset and slower recovery in SST,  
499 combined with a weak southern European climate response (see Fig. 5), is consistent with the  
500 modelling response of a St. Lawrence flood initiating the YD, but lake drainage from other  
501 sources and directions, such as the Mackenzie and Baltic, prolonging it. This is also  
502 consistent with the palaeohydrological reconstructions.

503 We now turn to Heinrich events, starting with H1. This was the main deglaciation iceberg  
504 release, which has a distinct and abrupt signature in the palaeo-records (Fig. 10), with the rise  
505 in sea level beginning c. 17.8k cal. yr B.P., approximately coinciding with abrupt fall in the  
506 Alboran Sea SST (f in Fig. 10), a decrease in the carbon content in runoff in Italy (g and h in  
507 Fig. 10), a fall in rainfall in the ITCZ proxy in Brazil and short-lived dips in Greenland  
508 temperature and Caribbean SST (\* in Fig. 10). These correspondences are consistent with a  
509 Hudson Strait iceberg release, particularly seen through the mid-latitude abrupt change but  
510 limited Greenland response (e.g. as seen in Fig. 5). However, the Alboran Sea SST shows a  
511 gradual, rather than abrupt, return over several hundred years to pre-event temperatures, with  
512 short-term coinciding temperature drops in Greenland (a in Fig. 10), the Caribbean and  
513 southern Europe during this period (g & h in Fig. 10). This contrast in rates of change  
514 between the beginning and end of H1, through comparison with the modelling results,  
515 suggest that H1 may have consisted of two events that affected climate: an initial Hudson  
516 Strait release followed by an Arctic or European release. The magnitude of the European  
517 signal suggests a possible Mackenzie source (Fig. 5). Several authors have found evidence  
518 for European IRD events preceding H1 (Grousset et al., 2000; Peck et al., 2006; Peck et al.,  
519 2007); there is also evidence for a Laurentide iceberg release into the Arctic about the same  
520 time as H1 (AL2; Darby et al., 2002). On the basis of the comparison of modelling and  
521 palaeo-records in Fig. 10, we hypothesise that any British-Irish Ice Sheet (BIIS) precursor to  
522 a Hudson Strait release was not large enough to have a significant climate impact, but that  
523 part of the North American response of the Laurentide ice sheet saw a later iceberg release  
524 enter the Arctic that continued the climate event associated with H1, leading to a slower  
525 recovery than there would otherwise have been.



526 The palaeoclimate data for the previous Heinrich event, H2, are shown in Fig. 11. The  
527 Atlantic SST data only begin during the event, so just the start of H2 is shown in these two  
528 fields (d & e in Fig. 11). However, across a wide number of variables onset of a cooling event  
529 is seen between 24.1-24.4k cal. yr B.P.. In most fields this onset is abrupt, with the majority  
530 of change occurring in less than 200 years. The exception is the Greenland temperature (a in  
531 Fig. 10), where there is relatively little impact. The bottom-sediment grain-size variable (c) is  
532 low throughout much of the interval; as will be seen repeatedly there is only a loose temporal  
533 association between this variable and what is occurring in the atmosphere and the surface  
534 ocean. The rising sea level (b in Fig. 11) suggests that iceberg loss continued until around  
535 23.3k cal. yr B.P.. The Greenland temperature, Mediterranean SST and Italian biogenic silica  
536 proxy all return to pre-event levels around this time, suggesting the recovery follows the  
537 cessation of enhanced iceberg flux quite quickly. This style of response is compatible with a  
538 predominantly Hudson Strait release, as H2 is normally considered to be (Hemming, 2004).  
539 However, the recovery in SST is slower than the initiation of change, which could be due to a  
540 climatic impact from the coinciding Arctic IRD event AL3 (Darby et al., 2002). Once again,  
541 the European H2 pre-cursor event identified by Scourse (2000), Grousset et al. (2001) and  
542 Peck et al. (2006) does not appear to have had a significant climatic impact.

543 H3, the selected palaeoclimate data for which are shown in Fig. 12, has long been seen as  
544 a problematic Heinrich event, with evidence of European source material in the eastern  
545 Atlantic, but of low concentration, and North American-sourced IRD in the west, but more  
546 abundant. Hemming (2004) summarises this evidence and concludes that H3 was of Hudson  
547 Strait origin, but of smaller size than other events, so that its IRD did not cover the North  
548 Atlantic, as in more characteristic events. One has a very different impression, however, from  
549 examining the palaeoclimate record, as there is a very strong and prolonged climate signal  
550 associated with this event. In all the temperature records in Fig. 12 there is a gradual decline  
551 of up to 5°C in SST (d, e & f in Fig. 12) and 10°C in Greenland air temperature (a in Fig. 12)  
552 during the interval 32-31k cal. yr B.P.; the MOC proxy (c in Fig. 12) is also lower during this  
553 interval. The end of this period is normally taken as the indicative time for H3 (Table 1),  
554 when the North Atlantic IRD signature is at its peak. A number of the records show some  
555 recovery around 30-30.5k cal. yr B.P., although in most cases it is centuries-long rather than  
556 abrupt. A full recovery of the Greenland air temperature and the SST fields, however, does  
557 not occur until c. 29k cal. yr B.P..

558 H3 therefore poses a problem – why is there so little IRD but such a strong climate  
559 anomaly? The nature of the anomaly suggests that despite the strong evidence for a regional  
560 IRD event originating from Hudson Strait there must have been some coincident or preceding  
561 cause of the major climate change. If this were due to an iceberg release then the slowness of  
562 the change suggests a European or Arctic origin. As Hemming (2004) shows, there is little  
563 evidence for a strong European source. However, Figures 2 and 7 of Darby et al. (2002) show  
564 that the maximum IRD signature during the last 35 000 years in core PS1230 from the Fram  
565 Strait occurred prior to 30k cal. yr B.P.. Their analysis was unable to link this peak with any  
566 of the source regions that they examined, and, in particular, it did not seem to be linked to  
567 Arctic North America. Our hypothesis to reconcile these various facts is that there was a  
568 major loss of ice from the Barents Sea ice shelf at this time, followed by a later, and smaller,  
569 Hudson Strait event. Lekens et al. (2006) show evidence in contemporary planktonic  
570 foraminiferal oxygen isotope anomalies of extensive meltwater across the surface of the  
571 whole Nordic Seas during H3, but little enhanced IRD flux at a core in the southern  
572 Norwegian Sea. This meltwater could have come from local sources as suggested by Lekens  
573 et al. (2006), but could also partially originate from melted Arctic icebergs (e.g., as seen in  
574 Fig. 4). Additional evidence for a significant IRD event originating from the eastern Arctic  
575 during H3 comes from core GC070 on the Yermak Plateau, NW of Svalbard and to the east  
576 of Fram Strait (Howe et al., 2008), where by far the largest IRD event recorded in this core  
577 during the main glacial period dates to around this time.

578 Fig. 13 shows the range of palaeodata around the time of H4. Just prior to 40k cal. yr B.P.  
579 there are abrupt changes in a number of indices, particularly eastern Atlantic SST (e in Fig.  
580 13), the ITCZ proxy in Brazil (i), the biogenic silica in Italy (h) and Greenland air  
581 temperature (a). At the same time, the sea level (b) begins to rise. These abrupt changes, and  
582 the relatively lesser response over Greenland, is consistent with the modelling results for a  
583 Hudson Strait iceberg release, which is normally considered the cause of H4 (Hemming,  
584 2004). The MOC proxy (c) also suggests weak return flow at this time, although the onset of  
585 this pre-dates the start of change elsewhere. The end of H4 is difficult to determine. The sea  
586 level ceases to rise around 39k cal. yr B.P. (b), shortly before Atlantic SST (e) and the MOC  
587 (c) return to more normal glacial conditions. However, the Mediterranean SST (f) and  
588 Greenland temperature (a) persist in an anomalous state for another 500 years before abrupt  
589 rises. This abruptness is consistent with the modelling results for a Hudson Strait recovery,  
590 however, the variable end point of the signal points to a more complex event. It is noteworthy

591 that at this same time there is evidence for changes in Antarctica, leading to the major sea  
592 level rise (Rohling et al., 2004), a Heinrich-like event and ice sheet collapse in the North  
593 Pacific (Bigg et al., 2008) and localised IRD events in the Nordic Seas (Dowdeswell et al.,  
594 1999). H4 may be part of a larger perturbation to the climate system.

595 In contrast to H3 and H4, the climate signal for H5 is hard to discern (Fig. 14). There are  
596 substantial amounts of IRD in the North Atlantic (Hemming, 2004) associated with this  
597 event, implying a Hudson Strait origin, but the Atlantic climate anomaly is small in the  
598 eastern Atlantic (e and b) to missing in the western Atlantic (d). There is a slow decline in the  
599 Alboran Sea SST (f) that correlates well with a decline in air temperature over Greenland (a),  
600 and the return to normal glacial conditions occurs around the same time in these two  
601 parameters, although much more abruptly over Greenland. However, these changes look  
602 more likely to be due to some other mechanism; H5 itself appears to have a weak climate  
603 impact, although one consistent in terms of rates of change with a Hudson Strait origin.

604 The final Heinrich event we consider is H6, which occurred around 60k cal. yr B.P.  
605 (Table 1). Hemming (2004) shows a number of IRD records associated with this event,  
606 although many suggest a much reduced flux (e.g. her Fig. 9). It is again difficult to see a  
607 significant climate signal in the proxy records chosen here (Fig. 15, although some (a & f in  
608 Fig. 15) do not extend this far back). There is a rise in sea level (b) around 60.7k cal. yr B.P.  
609 that may be associated with slight temperature falls in the Atlantic (d) and a reduced MOC  
610 (c), but the correspondence is weak.

611

## 612 **5. Discussion**

613 Comparison between a number of long term palaeoclimate records and modelling  
614 results for idealised releases of freshwater or icebergs into the Atlantic or Arctic Oceans has  
615 confirmed the important role of the Laurentide Ice Sheet in affecting glacial climate through  
616 ice and freshwater releases into the western Atlantic. Marine core evidence firmly points  
617 towards Hudson Strait as the primary origin of these releases (Hemming, 2004). However,  
618 the comparison has highlighted the variable climate impact of different Heinrich events, and  
619 hence likely differences between events in terms of iceberg release magnitude and/or  
620 duration. In addition, we have seen strong suggestions that other release areas have also  
621 played a role in producing the climate change observed in a number of events. In particular,  
622 past workers' concentration on the IRD record of the North Atlantic has tended to downplay  
623 the possibility of significant fluxes from Arctic sources. Few icebergs from the glacial Arctic

624 will have reached the main Atlantic basin to leave a lithic signature even from very large  
625 releases, because of the restriction of last glacial Arctic ice export to the narrow Fram Strait,  
626 and a long subsequent ocean passage through the Greenland Sea.

627         The rate of climate recovery from H1, H2 and H3 all suggested an Arctic release  
628 contribution to the climate impact. In the case of H1 and H2 we have seen that the IRD  
629 evidence from the Arctic and Fram Strait points towards a North American origin for a  
630 release coinciding with (or, in the case of H1, slightly later than) the Hudson Strait release.  
631 Darby et al. (2002)'s analysis of the FeO grain sizes in IRD suggests that Arctic event AL2  
632 (cf. H1) was largely Laurentide in origin, while AL3 (cf. H2) has a mix of Laurentide,  
633 Innuitian and North Greenland peaks. Stokes et al. (2005; 2009) suggest that the only likely  
634 source for a major Arctic Laurentide ice stream during this time interval was M'Clure Strait,  
635 roughly corresponding to one of our model release sites. In these two Heinrich events, even if  
636 there were a European pre-cursor as some authors have suggested, we hypothesise that the  
637 major climatic influence was due to a North American ice sheet collapse with both an eastern  
638 and northern signature.

639         H3 has a rather different character, however. While the model-data comparison  
640 suggests an Arctic component, the palaeoceanographic evidence suggests any release from  
641 the North American ice sheet c. 31k cal. yr B.P. was relatively minor, whether to the east  
642 (Hemming, 2004) or the north (Darby et al., 2002). Nevertheless, there was a strong  
643 meltwater signal in the Nordic Seas (Lekens et al., 2006), a strong IRD signal in Fram Strait  
644 at PS1230 (Darby et al., 2002) and a strong IRD signal off northern Svalbard at GC070  
645 (Howe et al., 2008). The combination of palaeoclimate and model evidence therefore points  
646 towards a release from the St. Anna Trough region being the dominant climate-altering cause  
647 of H3.

648         Earlier in the Last Glacial the Hudson Strait origin of Heinrich events H4, H5 and H6  
649 is clearer, with the IRD record in the Atlantic being consistent with the rates of change in the  
650 simulations. The Arctic also may have had a more constrained level of glaciation during this  
651 time (Svendsen et al., 2004). H6 had quite a small climate signal, consistent with the often  
652 weaker, and less widespread, IRD signal in the North Atlantic (Hemming, 2004). H4,  
653 however, had an unusual signature, with variable length of the climatic signal depending on  
654 location (Fig. 13). With evidence for widespread environmental change around this time  
655 elsewhere in the globe (Dowdeswell et al., 1999; Rohling et al., 2004; Bigg et al., 2008) we

656 suggest that this period merits further study to unravel the abrupt climate change occurring at  
657 this time.

658

### 659 **Acknowledgements**

660 This work was partially supported by the UK Natural Environmental Research Council Joint  
661 Rapid Climate Change programme through grant NE/C509523/1 and an e-Science  
662 studentship grant for CLG. We also wish to thank the IGBP PAGES/World Data Center for  
663 Paleoclimatology of the NOAA/NGDC Paleoclimatology Program, Boulder CO, USA for  
664 providing many of the palaeoclimate data sets. The original papers presenting these have  
665 been mentioned in the text. I would also like to thank Paul Coles for digitising two of the data  
666 sets where the original data were not available.

667

### 668 **References**

- 669 Allen, J.R.M., Brandt, U., Brauer, A., Hubberten, H.W., Huntley, B., Keller, J., Kraml, M.,  
670 Mackensen, A., Mingram, J., Negendank, J.F.W., Nowaczyk, N.R., Oberhänsli, H., Watts,  
671 W.A., Wulf, S., Zolitschka, B., 1999. Rapid environmental changes in southern Europe  
672 during the last glacial period. *Nature* 400, 740-743.
- 673 Alley, R.B., 2000. The Younger Dryas cold interval as viewed from central Greenland.  
674 *Quater. Sci. Rev.* 19, 213-226.
- 675 Bigg, G.R., Wadley, M.R., Stevens, D.P., Johnson, J.A., 1996. Prediction of iceberg trajectories  
676 for the North Atlantic and Arctic Oceans. *Geophys. Res. Lett.* 23, 3587-3590.
- 677 Bigg, G.R., Wadley, M.R., Stevens, D.P., Johnson, J.A., 1997. Modelling the dynamics and  
678 thermodynamics of icebergs. *Cold Regions Sci. Technol.* 26, 113-135.
- 679 Bigg, G.R., Wadley, M.R., 2001. The origin and flux of icebergs into the Last Glacial Maximum  
680 Northern Hemisphere Oceans. *J. Quater. Sci.* 16, 565-573.
- 681 Bigg, G.R., Clark, C.D., Hughes, A.L.C., 2008. A Last Glacial Ice Sheet on the Pacific Russian  
682 coast and catastrophic change arising from coupled ice-volcanic interaction. *Earth Planet. Sci*  
683 *Lett.* 265, 559-570.
- 684 Biscaye, P., Grousset, F., Revel, M., Van der Gaast, S., Zielinski, G., Vaars, A., Kukla, G.,  
685 1997. Asian provenance of glacial dust (stage 2) in the Greenland Ice Sheet Project 2 Ice  
686 Core, Summit, Greenland. *J. Geophys. Res.* 102(C12), 26765-26781.

687 Bond, G.C., Broecker, W.S., Johnsen, S., McManus, J.F., Labeyrie, L., Jouzel, J., Bonani, G.,  
688 1993. Correlation between climate records from North Atlantic sediments and Greenland  
689 ice. *Nature* 365, 143–147.

690 Bond, G.C., Showers, W., Elliot, M., Evans, M., Lotti, R., Hajdas, I., Bonani, G., Johnson, S.,  
691 1999. The North Atlantic's 1–2 kyr climate rhythm: relation to Heinrich events,  
692 Dansgaard/Oeschger cycles and the little ice age. In: Clark, P.U., Webb, R.S., Keigwin,  
693 L.D. (Eds.), *Mechanisms of Global Change at Millennial Time Scales*. American  
694 Geophysical Union, Washington DC. pp. 59–76.

695 Broecker, W.S., 1994. Massive iceberg discharges as triggers for global climate change.  
696 *Nature* 372, 421–424.

697 Broecker, W.S., Bond, G.C., Klas, M., Clark, E., McManus, J.F., 1992. Origin of the northern  
698 Atlantic's Heinrich events. *Clim. Dyn.* 6, 265–273.

699 Cacho, I., Grimalt, J.O., Pelejero, C., Canals, M., Sierro, F.J., Flores, J.A., Shackleton, N.J.,  
700 1999. Dansgaard-Oeschger and Heinrich event imprints in the Alboran Sea  
701 paleotemperatures. *Paleoceanogr.* 14, 698–705.

702 Calov, R., Ganopolski, A., Petoukhov, V., Claussen, M., Greve, R., 2002. Largescale  
703 instabilities of the Laurentide ice sheet simulated in a fully coupled climate-system model,  
704 *Geophys. Res. Lett.* 29, doi:10.1029/2002GL016078.

705 Cavalieri, D.J., Gloersen, P., Parkinson, C.L., Comiso, J.C., Zwally, H.J., 1997. Observed  
706 hemispheric asymmetry in global sea ice changes. *Science* 278, 1104 - 1106

707 Clement, A.C, Peterson, L.C., 2008. Mechanisms of abrupt climate change of the last glacial  
708 period. *Rev. Geophys.* 46, RG4002, doi:10.1029/2006RG000204.

709 Cruz, F.W.Jr., Burns, S.J., Karmann, I., Sharp, W.D., Vuille, M., Cardoso, A.O., Ferrari, J.A.,  
710 Silva Dias, P.L., Viana O.Jr., 2005. Insolation-driven changes in atmospheric circulation  
711 over the past 116,000 years in subtropical Brazil. *Nature* 434, 63–66.

712 Cuffey, K.M., Clow, G.D., 1997. Temperature, accumulation, and ice sheet elevation in  
713 central Greenland through the last deglacial transition. *J. Geophys. Res.* 102, 26383–  
714 26396.

715 Dansgaard, W., Johnsen, S.J., Clausen, H.B., Dahl-Jensen, D., Gundestrup, N.,  
716 Hammer, C.U., Oeschger, H., 1984. North Atlantic climatic oscillations revealed by deep  
717 Greenland ice cores, in *Climate Processes and Climate Sensitivity*. In: *Geophys. Monogr.*  
718 *Ser.*, vol. 29, Hansen, J.E., Takahashi, T., (Eds.). AGU, Washington, D.C., pp. 288–298.

719 Darby, D.A., Bischof, J.F., Spielhagen, R.F., Marshall, S.A., Herman, S.W., 2002. Arctic ice  
720 export events and their potential impact on global climate during the late Pleistocene.  
721 *Paleoceanogr.* 17, doi:10.1029/2001PA000639.

722 Darby, D.A., Zimmerman, P., 2008. Ice-rafted detritus events in the Arctic during the last  
723 glacial interval, and the timing of the Innuitian and Laurentide ice sheet calving events.  
724 *Polar Res.* 27, 114-127.

725 Death, R., Siegert, M.J., Bigg, G.R., Wadley, M.R., 2006. Modelling iceberg trajectories,  
726 sedimentation rates and meltwater input to the ocean from the Eurasian Ice Sheet at the Last  
727 Glacial Maximum. *Palaeogeogr., Palaeoclim. Palaeoecol.* 236, 135-150.

728 Dong, B., Valdes, P.J., 1998. Simulations of the Last Glacial Maximum climates using a  
729 general circulation model: Prescribed versus computed sea surface temperatures. *Clim.*  
730 *Dyn.* 14, 571–591.

731 Dowdeswell, J.A., Elverhøi, A., Andrews, J.T., Hebbeln, D., 1999. Asynchronous deposition  
732 of ice-rafted layers in the Nordic seas and North Atlantic Ocean. *Nature* 400, 348–351.

733 Fanning, A.F., Weaver, A.J., 1996. An atmospheric energy moisture-balance model:  
734 Climatology, interpentadal climate change and coupling to an OGCM. *J. Geophys. Res.*  
735 101, 15,111 – 15,128.

736 Farmer, L.G., Barber, D., Andrews, J., 2003. Provenance of Late Quaternary ice proximal  
737 sediments in the North Atlantic: Nd, Sr and Pb isotopic evidence. *Earth Planet. Sci. Lett.*  
738 209, 227– 243.

739 Fisher, T.G., 2003. Chronology of glacial Lake Agassiz meltwater routed to the Gulf of  
740 Mexico. *Quater. Res.* 59, 271–76.

741 Ganopolski, A., Rahmstorf, S., 2001. Rapid changes of glacial climate simulated in a coupled  
742 climate model. *Nature* 409, 153–158.

743 Gladstone, R., Bigg, G.R., Nicholls, K.W., 2001. Icebergs and fresh water fluxes in the Southern  
744 Ocean. *J. Geophys. Res.* 106, 19903-19915.

745 Gordon, A.L., 1986. Interocean exchange of thermocline water. *J. Geophys. Res.* 91 5037–  
746 5046.

747 Green, C.L., 2009. Modelling the impact of the glacial Barents Ice Shelf collapse, Ph. D.  
748 thesis, University of Sheffield.

749 Green, C.L., Bigg, G.R., Green, J.A.M., 2010. Deep draft icebergs from the Barents Ice Sheet  
750 during MIS6 are consistent with erosional evidence from the Lomonosov Ridge, central  
751 Arctic. *Geophys. Res. Lett.* 37, in press.

752 Grousset, F.E., Labeyrie, L., Sinko, J.A., Cremer, M., Bond, G., Duprat, J., Cortijo, E., Huon,  
753 S., 1993. Patterns of ice-rafted detritus in the glacial North Atlantic (40–55\_N),  
754 *Paleoceanogr.* 8, 175–192.

755 Grousset, F.E., Pujol, C., Labeyrie, L., Auffret, G., Boelaert, A., 2000. Were the North  
756 Atlantic Heinrich events triggered by the behavior of the European ice sheets? *Geol.* 28,  
757 123–126.

758 Grousset, F.E., Cortijo, E., Huon, S., Herve´, L., Richter, T., Burdloff, D., Duprat, J., Weber,  
759 O., 2001. Zooming in on Heinrich layers. *Paleoceanogr.* 16, 240–259.

760 Gwiazda, R.H., Hemming, S.R., Broecker, W.S., 1996a. Tracking the sources of icebergs  
761 with lead isotopes: The provenance of ice-rafted debris in Heinrich layer 2. *Paleoceanogr.*  
762 11, 77 – 93.

763 Gwiazda, R.H., Hemming, S.R., Broecker, W.S., 1996b. Provenance of icebergs during  
764 Heinrich event 3 and the contrast to their sources during other Heinrich episodes.  
765 *Paleoceanogr.* 11, 371 – 378.

766 Hansen, J., Sato, M., and many others 2007. Climate simulations for 1880-2003 with GISS  
767 model. *Clim. Dyn.* 29, 661-696.

768 Hemming, S., 2004. Heinrich events: Massive late Pleistocene detritus layers of the North  
769 Atlantic and their global climate imprint. *Rev. Geophys.* 42, RG1005,  
770 doi:10.1029/2003RG000128

771 Hoogakker, B.A., McCave, I.N., Vautravers, M.J., 2007. Antarctic link to deep flow speed  
772 variation during Marine Isotope Stage 3 in the western North Atlantic. *Earth Planet. Sci.*  
773 *Lett.* 257, 463-473.

774 Howe, J., Shimmield, T.M., Harland, R., 2008. Late Quaternary contourites and  
775 glaciomarine sedimentation in the Fram Strait. *Sedimentol.* 55, 179-200.

776 Kageyama, M., Laine, A., Abe-Ouchi A., Braconnot, P., Cortijo, E., Crucifix, M., de Vernal,  
777 A., Guiot, J., Hewitt, C.D., Kitoh, A., Kucera, M., Marti, O., Ohgaito, R., Otto-Bliesner,  
778 B., Peltier, W.R., Rosell-Mele, A., Vettoretti, G., Weber, S.L., Yu, Y. and MARGO  
779 Project Members, 2006. Last Glacial Maximum temperatures over the North Atlantic,  
780 Europe and western Siberia: a comparison between PMIP models, MARGO sea-surface  
781 temperatures and pollen-based reconstructions. *Quater. Sci. Rev.* 25, 2082-2102.

782 Kanfoush, S.L., Hodell, D.A., Charles, C.D., Guilderson, T.P., Mortyn, P.G., Ninnemann,  
783 U.S., 2000. Millennial-scale instability of the Antarctic Ice Sheet during the last  
784 glaciation. *Science* 288, 1815 – 1819.



785 Kristoffersen, Y., Coakley, B., Jokat, W, Edwards, M., Brekke, H/, Gjengedal, J., 2004.  
786 Seabed erosion on the Lomonosov Ridge, central Arctic Ocean: A tale of deep draft  
787 icebergs in the Eurasia Basin and the influence of Atlantic water inflow on iceberg  
788 motion? *Paleoceanogr.* 19, PA3006.

789 Kucera, M., Weinelt, M., Kiefer, T., Pflaumann, U., Hayes, A., Chen, M.T., Mix, A.C.,  
790 Barrows, T.T, Cortijo, E., Duprat, J., Juggins, S., Waelbroeck, C., 2005. Reconstruction  
791 of sea–surface temperatures from assemblages of planktonic foraminifera: multi-  
792 technique approach based on geographically constrained calibration data sets and its  
793 application to glacial Atlantic and Pacific Oceans. *Quater. Sci. Rev.* 24, 951–998.

794 Lea, D.W., Pak, D.K., Peterson, L.C., Hughen. K.A., 2003. Synchronicity of tropical and  
795 high-latitude Atlantic temperatures over the last glacial termination. *Science* 301,1361-  
796 1364.

797 Lekens W.A.H., Sejrup, H.P., Haflidason, H., Knies, J., Richter, T., 2006. Meltwater and ice  
798 rafting in the southern Norwegian Sea between 20 and 40 calendar kyr B.P.: Implications  
799 for Fennoscandian Heinrich events. *Paleoceanogr.* 21, PA3013,  
800 doi:10.1029/2005PA001228.

801 Lekens, W.A.H., Haflidason, H., Sejrup, H.P., Nygard, A., Richter, T., Vogt, C., Frederichs,  
802 T., 2009. Sedimentation history of the northern North Sea margin during the last 150 ka.  
803 *Quater. Sci. Rev.* 28, 469-483.

804 Leverington, D.W., Teller, J.T., 2003. Paleotopographic reconstructions of the eastern outlets  
805 of glacial Lake Agassiz. *Can. J. Earth Sci.* 40, 1259–78.

806 Levine, R.C., Bigg, G.R., 2008. The sensitivity of the glacial ocean to Heinrich events from  
807 different sources, as modeled by a coupled atmosphere-iceberg-ocean model.  
808 *Paleoceanogr.* 23, PA4213, doi:10.1029/2008PA001613.

809 MacAyeal, D.R., 1993. Binge/purge oscillations of the Laurentide ice sheet as a cause of the  
810 North Atlantic’s Heinrich events. *Paleoceanogr.* 8, 775 – 784.

811 Macrander, A., Send, U., Valdimarsson, H., Jónsson, S., Käse, R.H., 2005. Interannual  
812 changes in the overflow from the Nordic Seas into the Atlantic Ocean through Denmark  
813 Strait. *Geophys. Res. Lett.* 32, doi:10.1029/2004GL021463.

814 McCave, I.N., Manighetti, B., Robinson, S.G., 1995. Sortable silt and fine sediment  
815 size/composition slicing: parameters for palaeocurrent speed and palaeoceanography.  
816 *Paleoceanogr.* 10, 593–610.

817 McCave, I.N., Hall, I.R., 2006. Size sorting in marine muds: processes, pitfalls and prospects  
818 for paleoflow-speed proxies. *Geochem. Geophys. Geosyst.* 7,  
819 doi:10.1029/2006GC001284.

820 Murton, J.B., Bateman, M.D., Dallimore, S.R., Teller, J.T., Yang, Z., 2010. Mackenzie  
821 outburst flooding into the Arctic Ocean at the start of the Younger Dryas. *Nature* 464,  
822 740-743.

823 Nesje, A., Dahl, S., Bakke, J., 2004. Were abrupt Lateglacial and early-Holocene climatic  
824 changes in northwest Europe linked to freshwater outbursts to the North Atlantic and  
825 Arctic Oceans? *Holocene* 14, 299-310.

826 Nygård A., Sejrup, H.P., Haflidason, H., Lekens, W.A.H., Clark, C.D., Bigg, G.R., 2007.  
827 Extreme sediment and ice discharge from marine-based ice streams: New evidence from  
828 the North Sea. *Geol.* 35, 395-398.

829 Nowlin, W.D., Klinck, J.M., 1986. The physics of the Antarctic circumpolar current. *Rev.*  
830 *Geophys.* 23, 459–491.

831 Østerhus, S., Turrell, W.R., Jónsson, S., Hansen, B., 2005. Measured volume, heat, and salt  
832 fluxes from the Atlantic to the Arctic Mediterranean. *Geophys. Res. Lett.* 32,  
833 doi:10.1029/2004GL022188.

834 Peck, V.L., Hall, I.R., Zahn, R., Elderfield, H., Grousset, F., Hemming, S.R., Scourse, J.D.,  
835 2006. High resolution evidence for linkages between NW European ice sheet instability  
836 and Atlantic meridional overturning circulation. *Earth Planet. Sci. Lett.* 243, 476–481.

837 Peck, V.L., Hall, I.R., Zahn, R., Grousset, F., Hemming, S.R., Scourse, J.D., 2007. The  
838 relationship of Heinrich events and their European precursors over the past 60ka BP: a  
839 multi-proxy ice-rafted debris provenance study in the North East Atlantic. *Quater. Sci.*  
840 *Rev.* 26, 862-875.

841 Peltier, W.R., 1994. Ice-age paleotopography. *Science* 265, 195 – 201.

842 Pflaumann, U., Sarnthein, M., Chapman, M., d'Abreu, L., Funnell, B., Huels, M., Kiefer, T.,  
843 Maslin, M.A., Schulz, H., Swallow, J., van Kreveld, S., Vautravers, M., Vogelsang, E.,  
844 Weinelt, M., 2003. Glacial North Atlantic: Sea-surface conditions reconstructed by  
845 GLAMAP 2000. *Paleoceanogr.* 18, doi:10.1029/2002PA000774.

846 Piper, D.J.W., Skene, K.I., 1998. Latest Pleistocene ice-rafting events on the Scotian margin  
847 (eastern Canada) and their relationship to Heinrich events. *Paleoceanogr.* 13, 205-214.

848 Piper, D.J.W., DeWolfe, M., 2003. Petrographic evidence from the eastern Canadian margin  
849 of shelf-crossing glaciations. *Quater. Int.* 99, 99-113.

850 Polyak, ., Forman, S.L., Herlihy, F.A., Ivanov, G., Krinitsky, P., 1997. Late Weichselian  
851 deglacial history of the Svyataya (Saint) Anna Trough, northern Kara Sea, Arctic Russia.  
852 *Mar. Geol.* 143, 169-188.

853 Rind, D., deMenocal, P., Russell, G., Sheth, S., Collins, D., Schmidt, G., Teller, J., 2001.  
854 Effects of glacial meltwater in the GISS coupled atmosphere ocean model: 1. North  
855 Atlantic Deep Water response. *J. Geophys. Res.* 106(D21), 27,335–27,353.

856 Roche, D., Paillard, D., Cortijo, E., 2004. Constraints on the duration and freshwater release  
857 of Heinrich event 4 through isotope modelling. *Nature* 432, 379 – 382.

858 Rohling, E.J., Marsh, R., Wells, N.C., Siddall, M., Edwards, N.R., 2004. Similar meltwater  
859 contributions to glacial sea level changes from Antarctic and northern ice sheets. *Nature*  
860 430, 1016-1021.

861 Rogerson, M., Colmenero-Hidalgo, E., Levine, R.C., de Abreu, L., Rohling, E.J., Voelker,  
862 A.H.L., Bigg, G.R., Schönfeld, J., Cacho, I., Sierro, F.J., Löwemark, L., Reguera, M.I., de  
863 Abreu, L., Garrick, K., 2010. Enhanced Mediterranean-Atlantic exchange during Atlantic  
864 freshening phases. *Geochem., Geophys., Geosys.* 11, Q08013,  
865 doi:10.1029/2009GC002931.

866 Schmitz, W.J., 1995. On the interbasin-scale thermohaline circulation. *Rev. Geophys.* 33,  
867 151–173.

868 Scourse, J.D., Hall, I.R., McCave, I.N., Young, J.R., Sugdon, C., 2000. The origin of  
869 Heinrich layers: Evidence from H2 for European precursor events. *Earth Planet. Sci. Lett.*  
870 182, 187–195.

871 Seidov, D., Maslin, M., 1999. North Atlantic deep water circulation collapse during Heinrich  
872 events. *Geol.* 27, 23-26.

873 Sejrup, H.P., Nygard, A., Hall, A.M., Haflidason, H., 2009. Middle and Late Weichselian  
874 (Devensian) glaciation history of south-western Norway, North Sea and eastern UK.  
875 *Quater. Sci. Rev.* 28, 370-380.

876 Siddall, M., Rohling, E.J., Almogi-Labin, A., Hemleben, C., Meischner, D., Schmelzer, I.,  
877 Smeed, D.A., 2003. Sea-level fluctuations during the last glacial cycle. *Nature* 423, 853-  
878 858.

879 Stokes, C.R., Clark, C.D., Darby, D.A., Hodgson, D.A., 2005, Late Pleistocene ice export  
880 events into the Arctic Ocean from the M'Clure Strait Ice Stream, Canadian Arctic  
881 Archipelago. *Glob. Planet. Change* 49, 139-162.

882 Stokes, C.R., Clark, C.D., Storrar, R., 2009. Major changes in ice stream dynamics during  
883 deglaciation of the north-western margin of the Laurentide Ice Sheet. *Quater. Sci. Rev.*  
884 28, 721-738.

885 Stouffer, R.J., et al., 2006. Investigating the causes of the response of the thermohaline  
886 circulation to past and future climate changes. *J. Clim.* 19, 1365 – 1387.

887 Svendsen, J.I., et al. 2004. Late quaternary ice sheet history of northern Eurasia. *Quater. Sci.*  
888 *Rev.* 23, 1229-1271.

889 Teller, J.T., Leverington, D.W., Mann, J.D., 2002. Freshwater outbursts to the oceans from  
890 glacial Lake Agassiz and their role in climate change during the last deglaciation. *Quater.*  
891 *Sci. Rev.* 21, 879-887.

892 Timmermann, Gildor, H., Schulz, M., Tziperman, E., 2003. Coherent resonant millennial-  
893 scale climate oscillations triggered by massive meltwater pulses. *J. Clim.* 16, 2569-2585.

894 Tomczak, M., Godfrey, J.S., 2003. *Regional Oceanography: an Introduction*. 2nd ed., Daya,  
895 Delhi, 390pp.

896 Vautravers, M.J., Shackleton, N.J., Lopez-Martinez, C., Grimalt, J.O., 2004. Gulf Stream  
897 variability during marine isotope stage 3. *Paleoceanogr.* 19, PA2011,  
898 doi:10.1029/2003PA000966.

899 Vautravers, M.J., Shackleton, N.J., 2006. Centennial-scale surface hydrology off Portugal  
900 during marine isotope stage 3: Insights from planktonic foraminiferal fauna variability.  
901 *Paleoceanogr.* 21, PA3004, doi:10.1029/2005PA001144.

902 Vellinga, M., Wood, R.A., 2002. Global climatic impacts of a collapse of the Atlantic  
903 thermohaline circulation. *Clim. Change* 54, 251–267.

904 Voelker, A.H.L., 2002). Global distribution of centennial-scale records for Marine Isotope  
905 Stage (MIS) 3: a database. *Quater. Sci. Rev.* 21, 1185–1212.

906 Wadley, M.R., Bigg, G.R., 1999. Implementation of variable time stepping in an ocean  
907 general circulation model. *Ocean Modell.* 1, 71– 80.

908 Wadley, M.R., Bigg, G.R., 2002. Impact of flow through the Canadian Archipelago on the  
909 North Atlantic and Arctic thermohaline circulation: an ocean modelling study. *Quart. J. Roy.*  
910 *Meteor. Soc.* 128, 2187-2203.

911 Webb, D.J., 1996. An ocean model code for array processor computers. *Comput. Geophys.*  
912 22, 569– 578.

913 Weber, S.L., Drijfhout, S.S., Abe-Ouchi, A., Crucifix, M., Eby, M., Ganopolski, A.,  
914 Murakami, S., Otto-Bliesner, B., Peltier, W.R., 2007. The modern and glacial overturning  
915 circulation in the Atlantic Ocean in PMIP coupled model simulations. *Clim. Past* 3, 51-64.  
916

917 **Table 1**  
 918 Approximate ages (calendar years BP) of the start of the abrupt events considered here.  
 919 Hemming (2004) gives estimates of the uncertainty in H3 of  $\pm 1000$  years and H6 of  $\pm 5000$   
 920 years. Our estimate comes from the timing of disturbance in the Northern Atlantic and  
 921 represents the mid-point of the event ( $\pm 250$  years).

Event	Hemming (2004) Age (BP)	Estimated Age (BP) here
Younger Dryas	12 900	12 600
H1	16 800	17 500
H2	24 000	24 000
H3	31 000	31 000 <sup>a</sup>
H4	38 000	39 200
H5	45 000	46 100
H6	60 000	60 000

922 <sup>a</sup>H3 appears to be unusually prolonged from a number of records.

923 **Figure Legends**

924 **Fig. 1.** High temporal resolution records spanning the last 50 000 years of GISP2 Greenland  
925 ice core temperature (bottom panel; data from Alley (2000)), Alboran Sea surface  
926 temperature (centre panel; data from Cacho et al. (1999)) and Italian lake sediment biogenic  
927 silica (top panel; data from Allen et al. (1999)). Note the fast rates of change and the  
928 variations in amplitude and frequency in the records.

929 **Fig. 2.** Iceberg and fresh water release sites for a glacial Arctic. A schematic of model annual  
930 mean glacial ocean currents is also shown.

931 **Fig. 3.** MOC strength (in Sv) for 500 year iceberg releases of 0.1 (dashed), 0.2 (dot-dashed),  
932 0.4 (solid) Sv from the 5 sites, clockwise around the Atlantic and Arctic from bottom to top.  
933 The control MOC variation over this time is shown by the dotted line in each segment.

934 **Fig. 4.** Sea surface salinity at model Year 5800 (ie 300 years into an iceberg release) for the  
935 following experiments: Control (bottom right), and 0.4 Sv iceberg releases for the St.  
936 Lawrence (bottom left), Hudson Strait (centre left), MacKenzie (top left), St. Anna Trough  
937 (top right) and NCIS (centre right). Absolute values are shown for the Control but anomalies  
938 relative to the Control for all other experiments. Contours are every 0.5, with labels at integer  
939 values. The data have been transformed onto a 1 degree conventional latitude-longitude grid,  
940 so there is a slight discrepancy between the model ocean data (land shown in white) and  
941 modern day land boundaries relative to a zero height at the 123m bathymetric contour (shown  
942 in black).

943 **Fig. 5.** Lower atmospheric temperatures at model Year 5800 (ie 300 years into an iceberg  
944 release) for the following experiments: Control (bottom right), and 0.4 Sv iceberg releases for  
945 the St. Lawrence (bottom left), Hudson Strait (centre left), MacKenzie (top left), St. Anna  
946 Trough (top right) and NCIS (centre right). Absolute values are shown for the Control but  
947 anomalies relative to the Control for all other experiments. Contours are every 5°C for the  
948 Control and 0.5°C for the anomalies, with labels at integer values for the latter. The darker  
949 shading shows the more negative contours for the anomaly plots. The modern day land  
950 boundaries, relative to a zero height at the 123m bathymetric contour, are shown hatched.

951 **Fig. 6.** MOC strength (in Sv) for 500 year freshwater releases of 0.1 (dashed), 0.2 (dot-  
952 dashed), 0.4 (solid) Sv from the 5 sites, clockwise around the Atlantic and Arctic from  
953 bottom to top. The control MOC variation over this time is shown by the dotted line in each  
954 segment. Note that the 0.4 Sv releases from the two European sites led to numerical  
955 instabilities, while the 0.2 Sv release from the NCIS, while complete, was also affected by  
956 numerical problems.

957 **Fig. 7.** Map of sites for palaeoclimate data, mostly labelled as in Fig. 8 (a-b, e-f, and i) or Fig.  
958 9 (\*). Note that data sets c and d from Fig. 8 are from the same marine core in the sub-  
959 tropical west Atlantic, so this site is labelled “W”, and sets g & h are from the same lake in  
960 southern Italy, hence labelled “L”. Dataset \* is only used for the Younger Dryas comparison  
961 (see Fig. 9).

962 **Fig. 8.** Plot of palaeoclimate datasets on a common timescale. From the bottom up there is a  
963 a Greenland ice core temperature (Alley, 2000), b) a sea level record (Siddall et al., 2003), c)  
964 an MOC sortable silt index (Hoogakker et al., 2007), d) a western Atlantic SST (Vautravers  
965 et al., 2004), e) an eastern Atlantic SST (Vautravers and Shackleton, 2006), f) a western  
966 Mediterranean SST (Cacho et al., 1999), g) a terrestrial organic carbon record (Allen et al.,  
967 1999), h) a terrestrial biogenic silica record (Allen et al., 1999), and i) a speleotherm  $\delta^{18}\text{O}$   
968 record (Cruz et al., 2005). See Fig. 7 for a key as to the location of the different datasets.

969 **Fig. 9.** Comparison of palaeoclimate records during a time interval focused on the Younger  
970 Dryas (c. 12.5ka). The panels are labelled to correspond to the locations shown on Fig. 7. See  
971 the longer sets of timeseries, of which this is an excerpt, in Fig. 8, except for the Caribbean  
972 SST record (\*, Lea et al., 2003).

973 **Fig. 10.** Comparison of palaeoclimate records during a time interval focused on H1 (c.  
974 18ka). The panels are labelled to correspond to the locations shown on Fig. 7. See the longer  
975 sets of timeseries, of which this is an excerpt, in Fig. 8, except for the Caribbean SST record  
976 (\*).

977 **Fig. 11.** Comparison of palaeoclimate records during a time interval focused on H2 (c.  
978 24ka). The panels are labelled to correspond to the locations shown on Fig. 7. See the longer  
979 sets of timeseries, of which this is an excerpt, in Fig. 8.

980 **Fig. 12.** Comparison of palaeoclimate records during a time interval focused on H3 (c.  
981 31ka). The panels are labelled to correspond to the locations shown on Fig. 7. See the longer  
982 sets of timeseries, of which this is an excerpt, in Fig. 8.

983 **Fig. 13.** Comparison of palaeoclimate records during a time interval focused on H4 (c.  
984 40ka). The panels are labelled to correspond to the locations shown on Fig. 7. See the longer  
985 sets of timeseries, of which this is an excerpt, in Fig. 8.

986 **Fig. 14.** Comparison of palaeoclimate records during a time interval focused on H5 (c.  
987 46ka). The panels are labelled to correspond to the locations shown on Fig. 7. See the longer  
988 sets of timeseries, of which this is an excerpt, in Fig. 8.

989 **Fig. 15.** Comparison of palaeoclimate records during a time interval focused on H6 (c.  
990 61ka). The panels are labelled to correspond to the locations shown on Fig. 7. See the longer  
991 sets of timeseries, of which this is an excerpt, in Fig. 8.

992



Figure 1  
[Click here to download high resolution image](#)

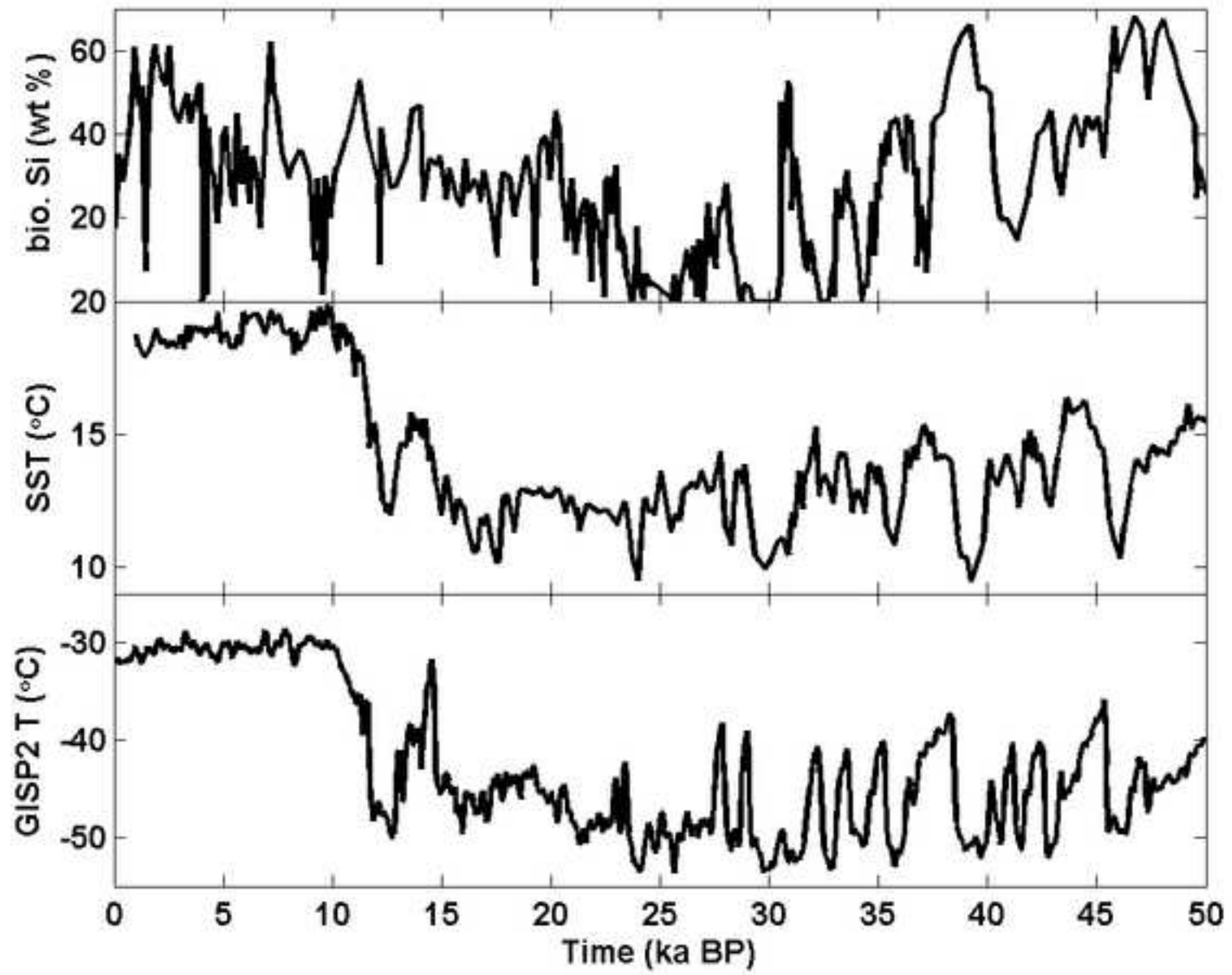


Figure 2  
[Click here to download high resolution image](#)

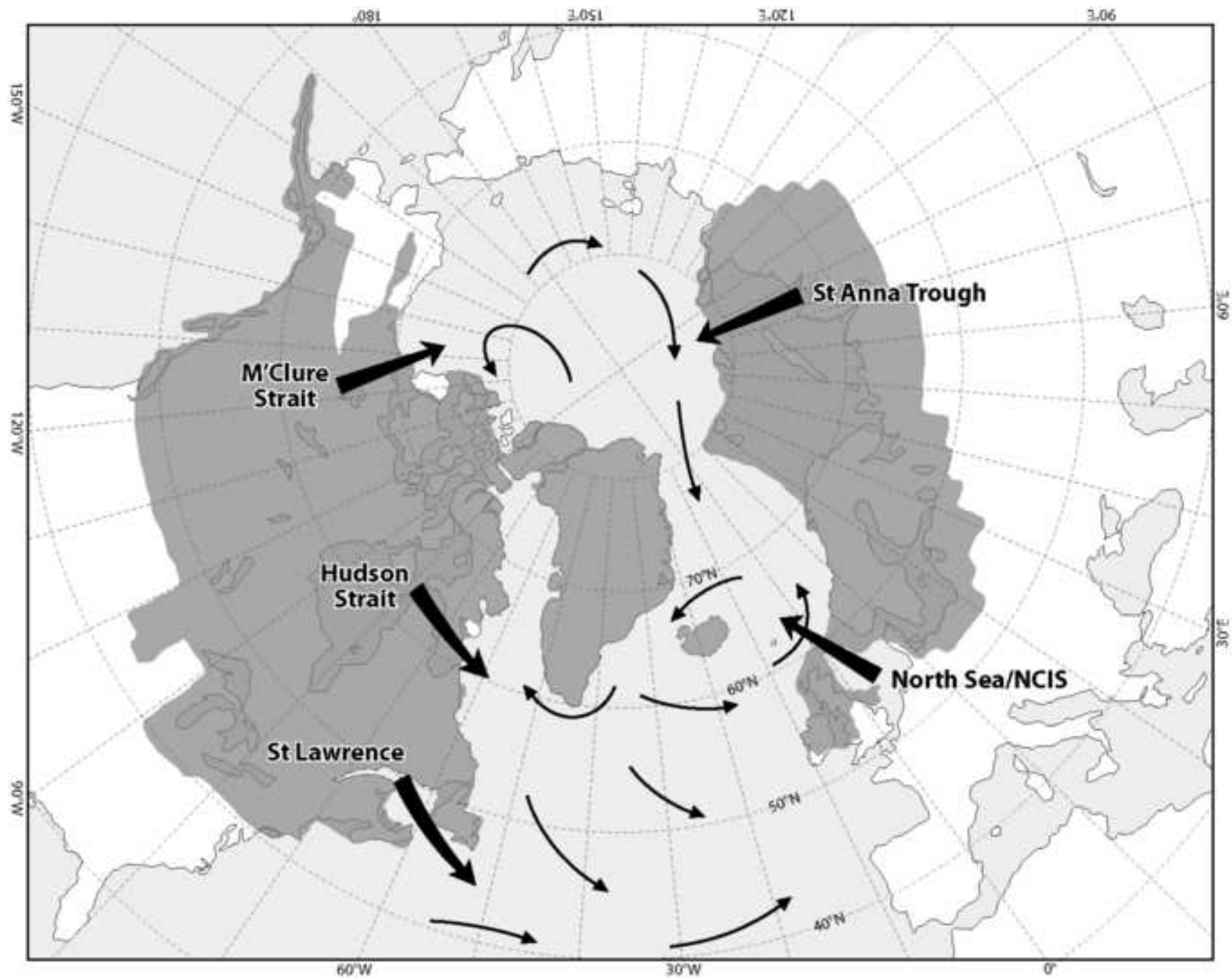


Figure 3  
[Click here to download high resolution image](#)

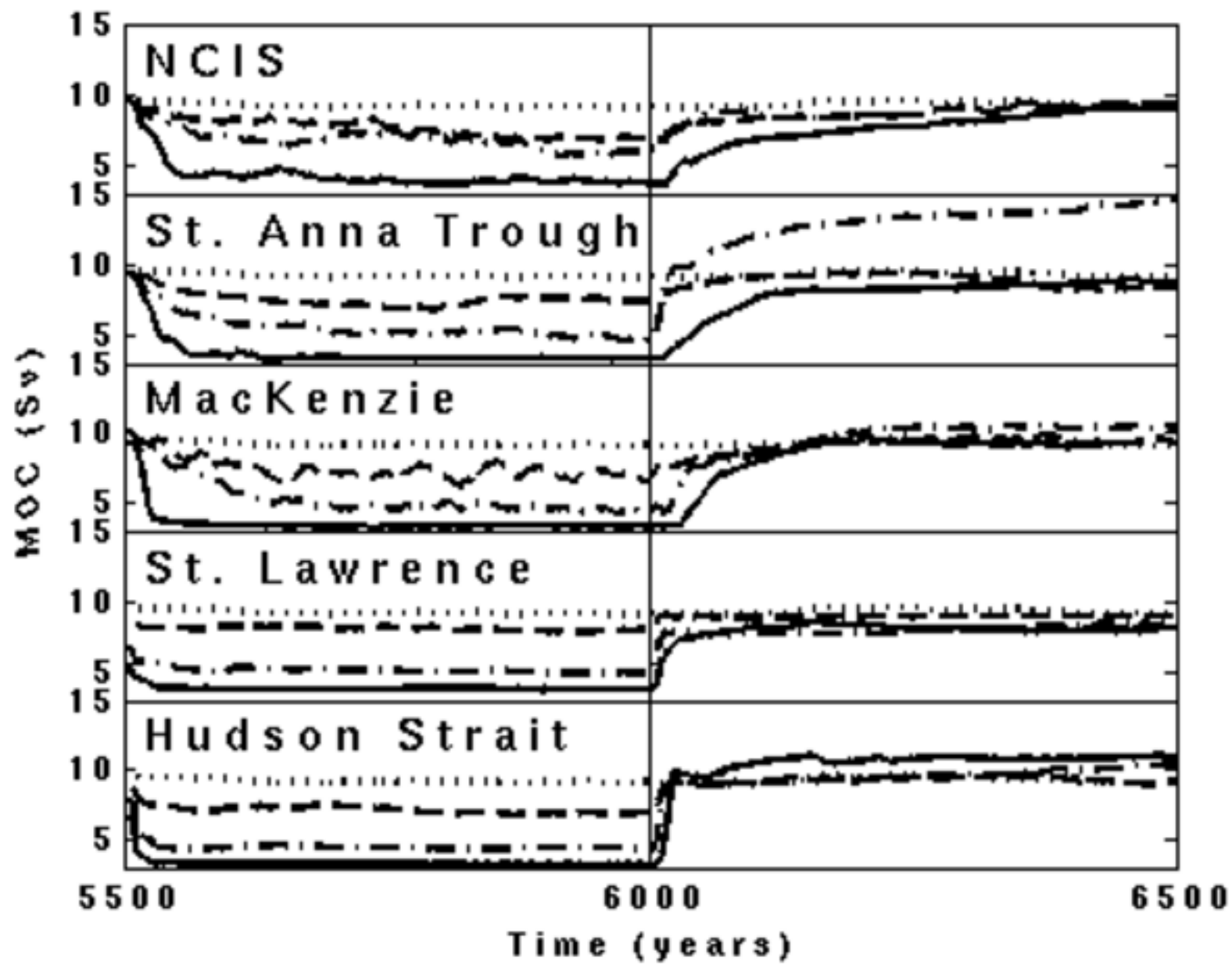


Figure 4  
[Click here to download high resolution image](#)

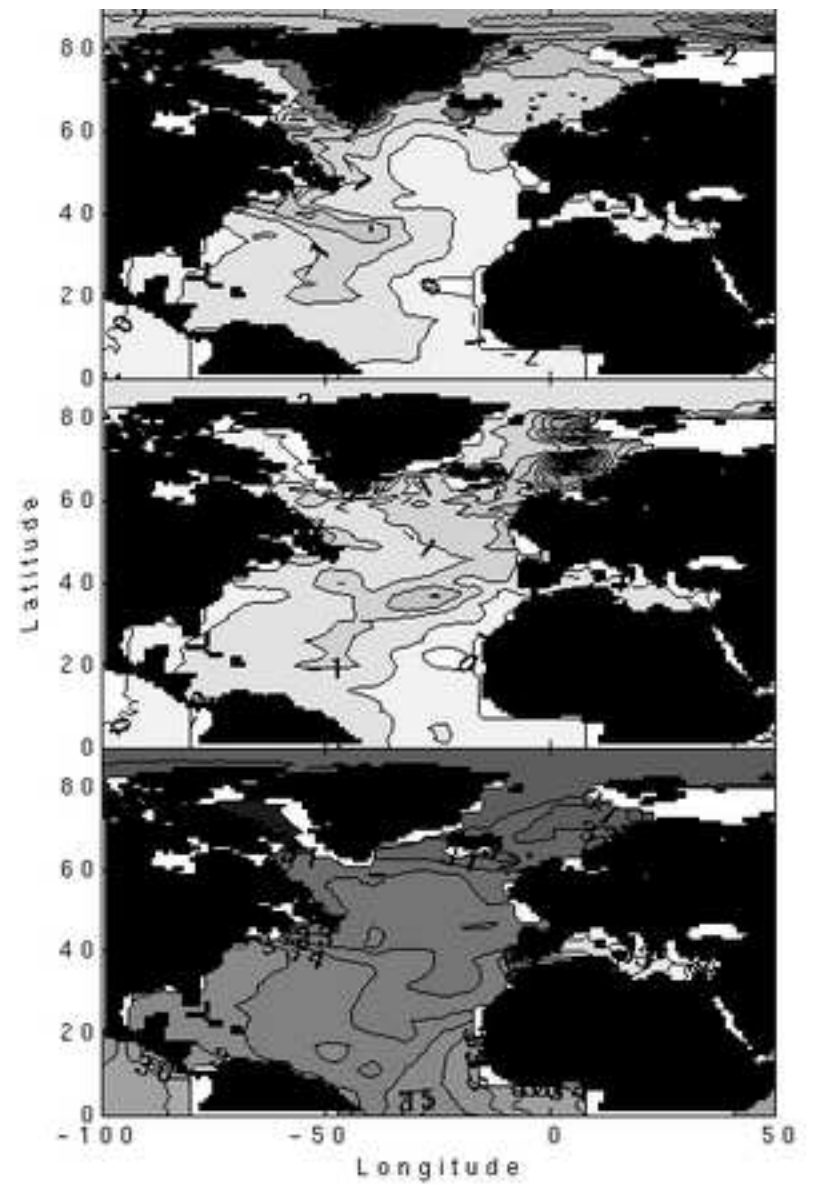
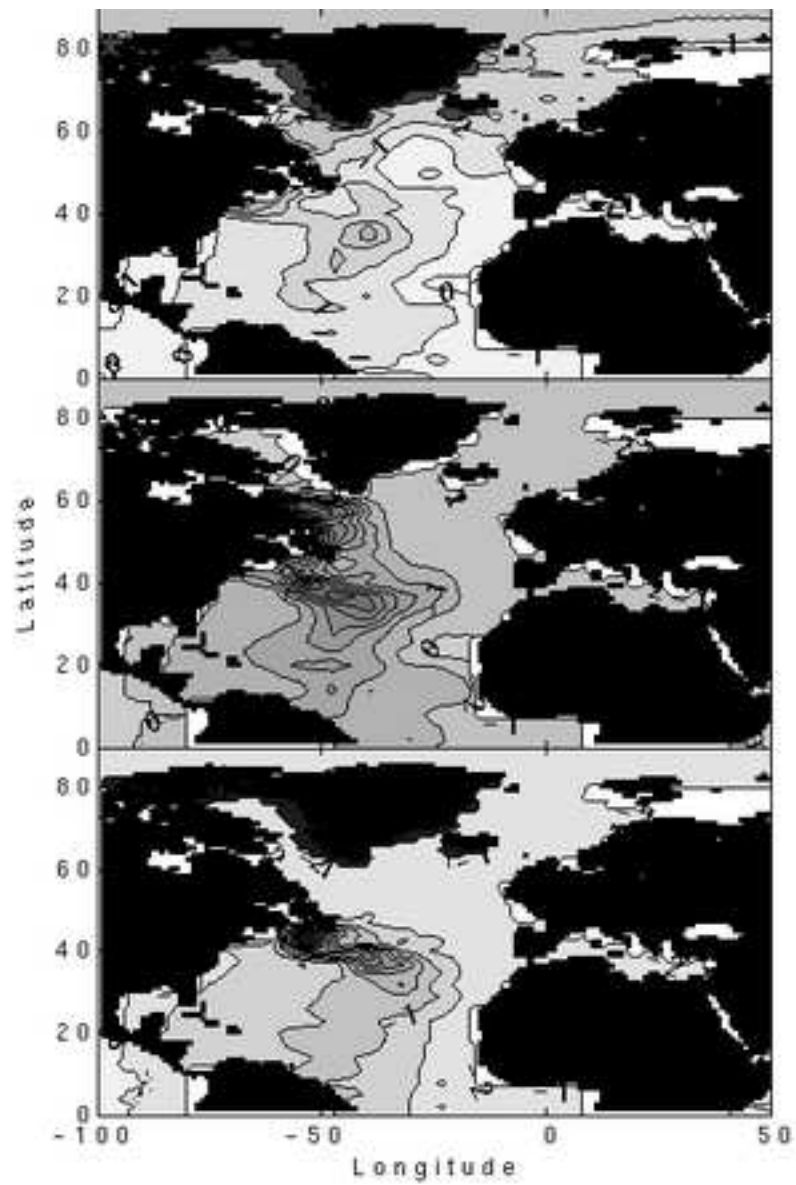


Figure 5

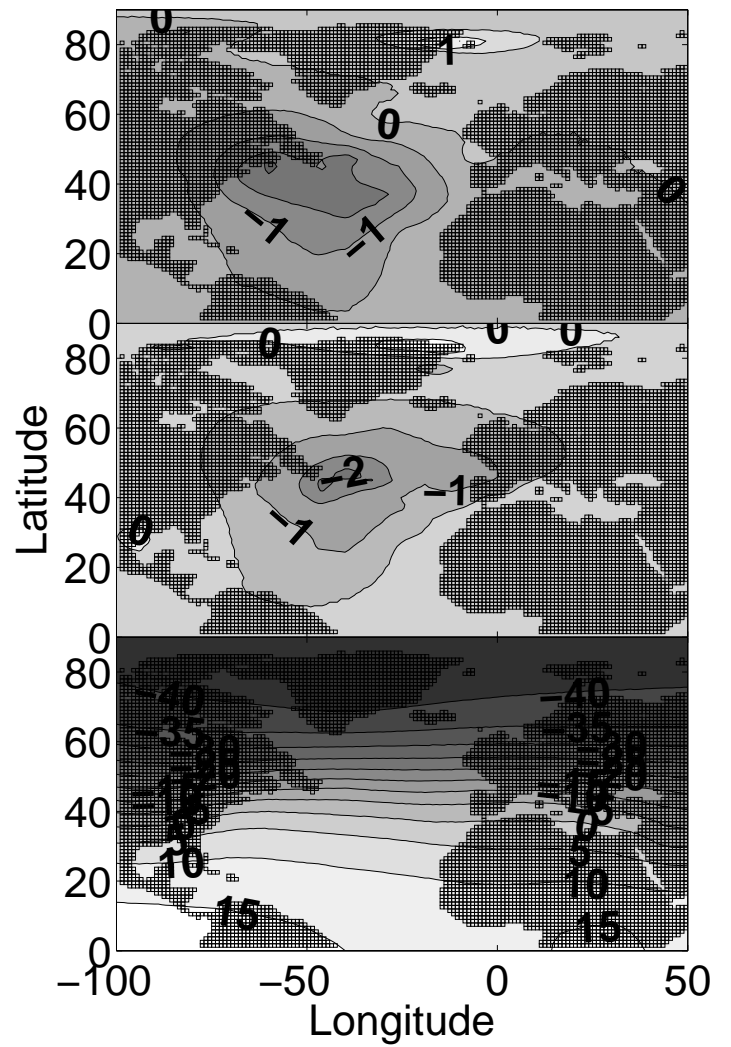
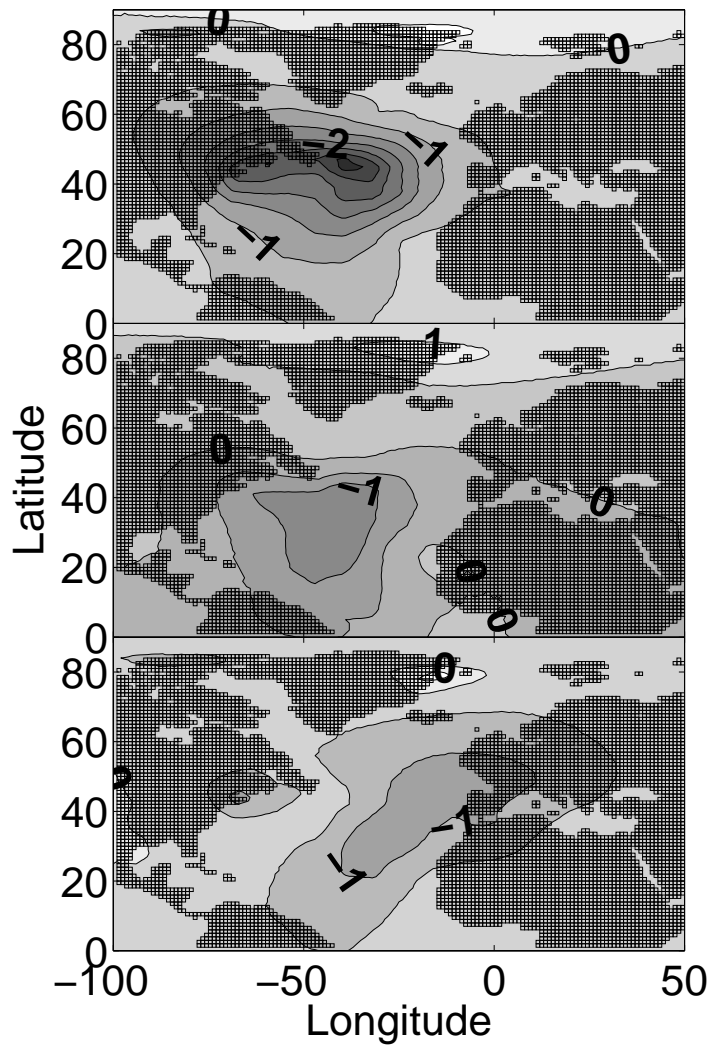


Figure 6

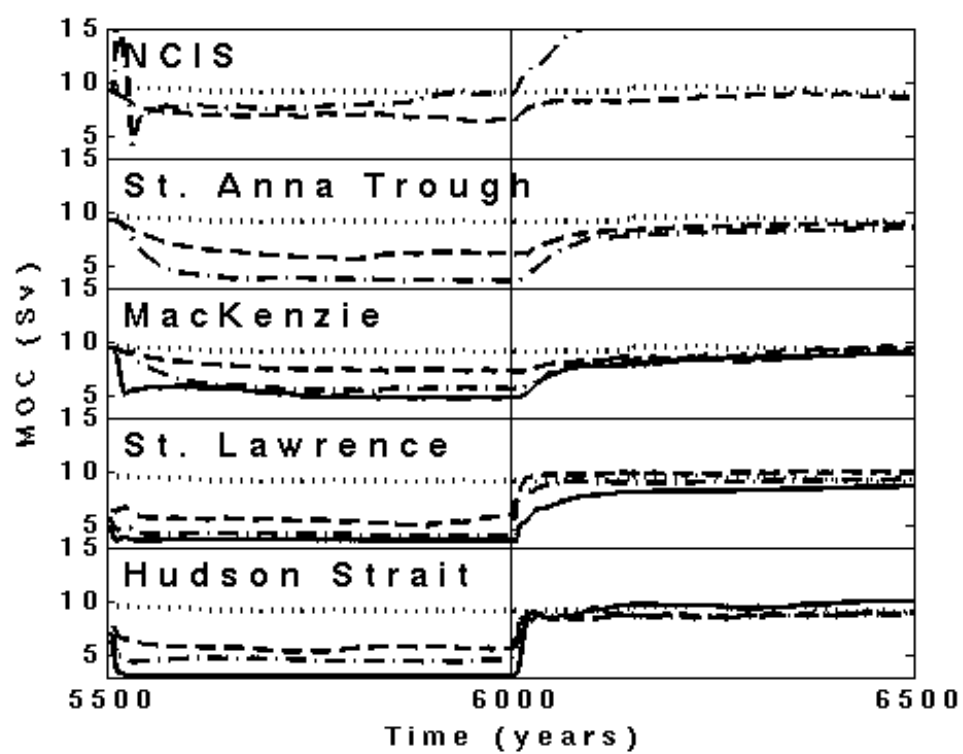




Figure 7  
[Click here to download high resolution image](#)

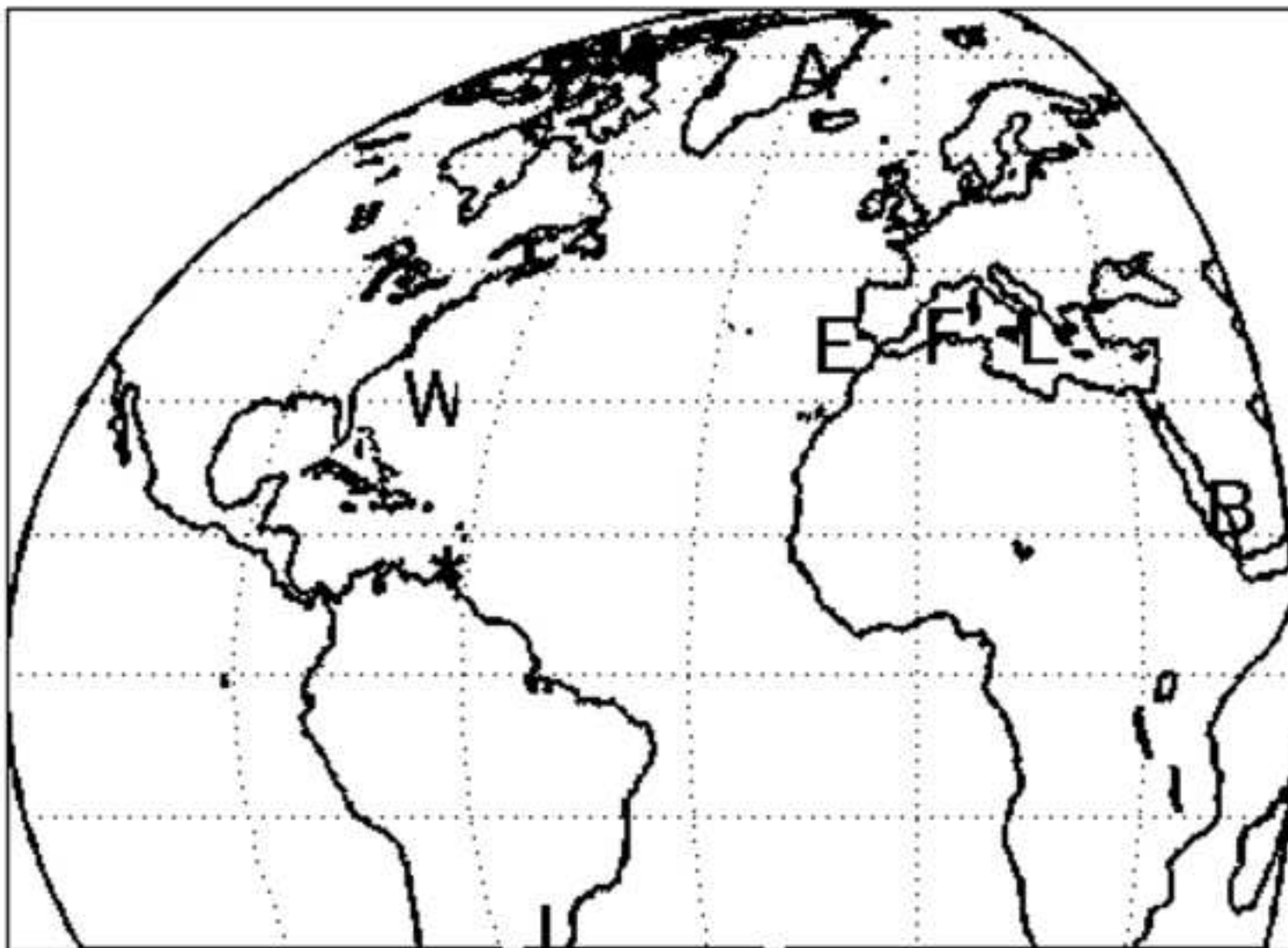


Figure 8  
[Click here to download high resolution image](#)

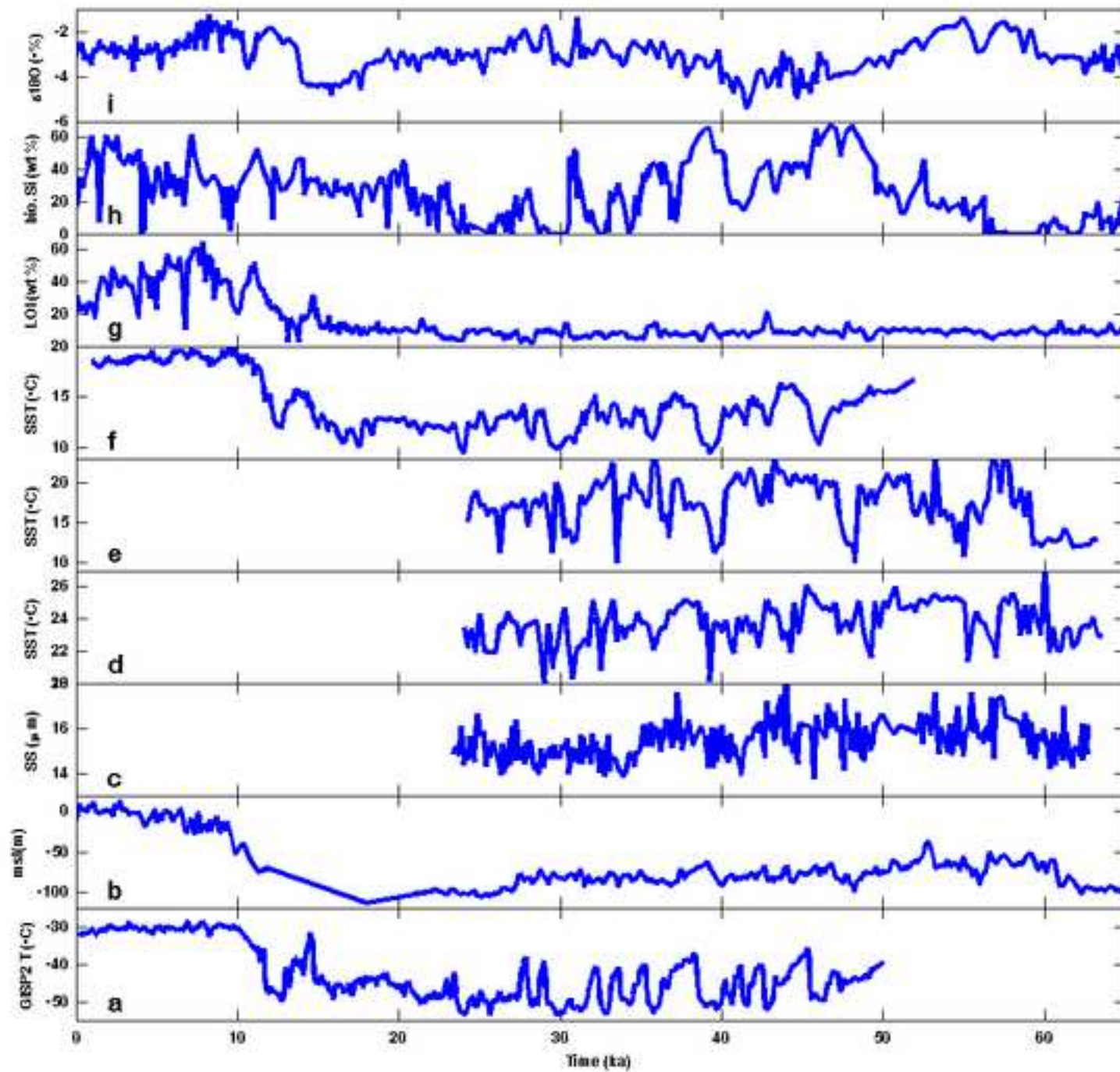




Figure 9  
[Click here to download high resolution image](#)

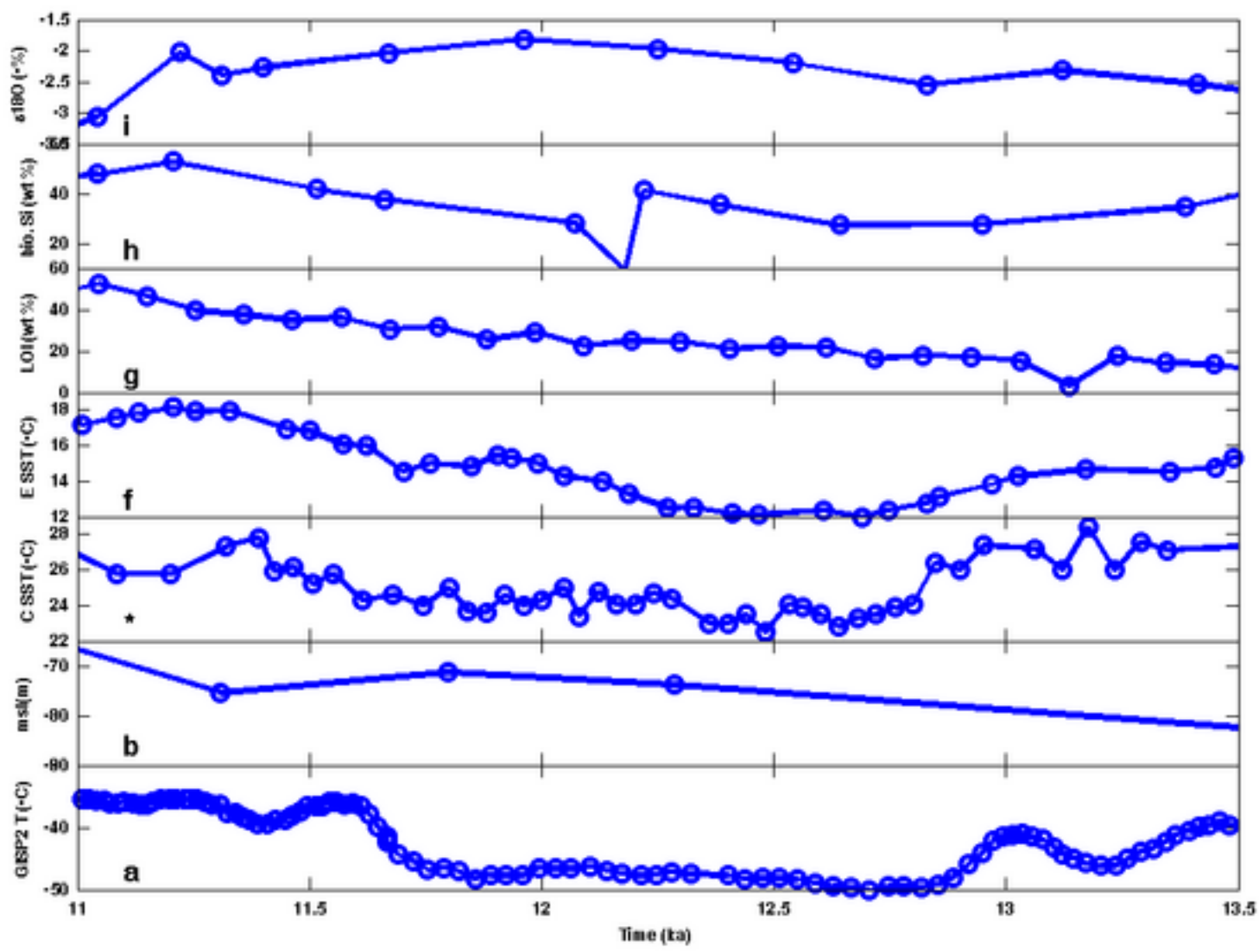


Figure 10

[Click here to download high resolution image](#)

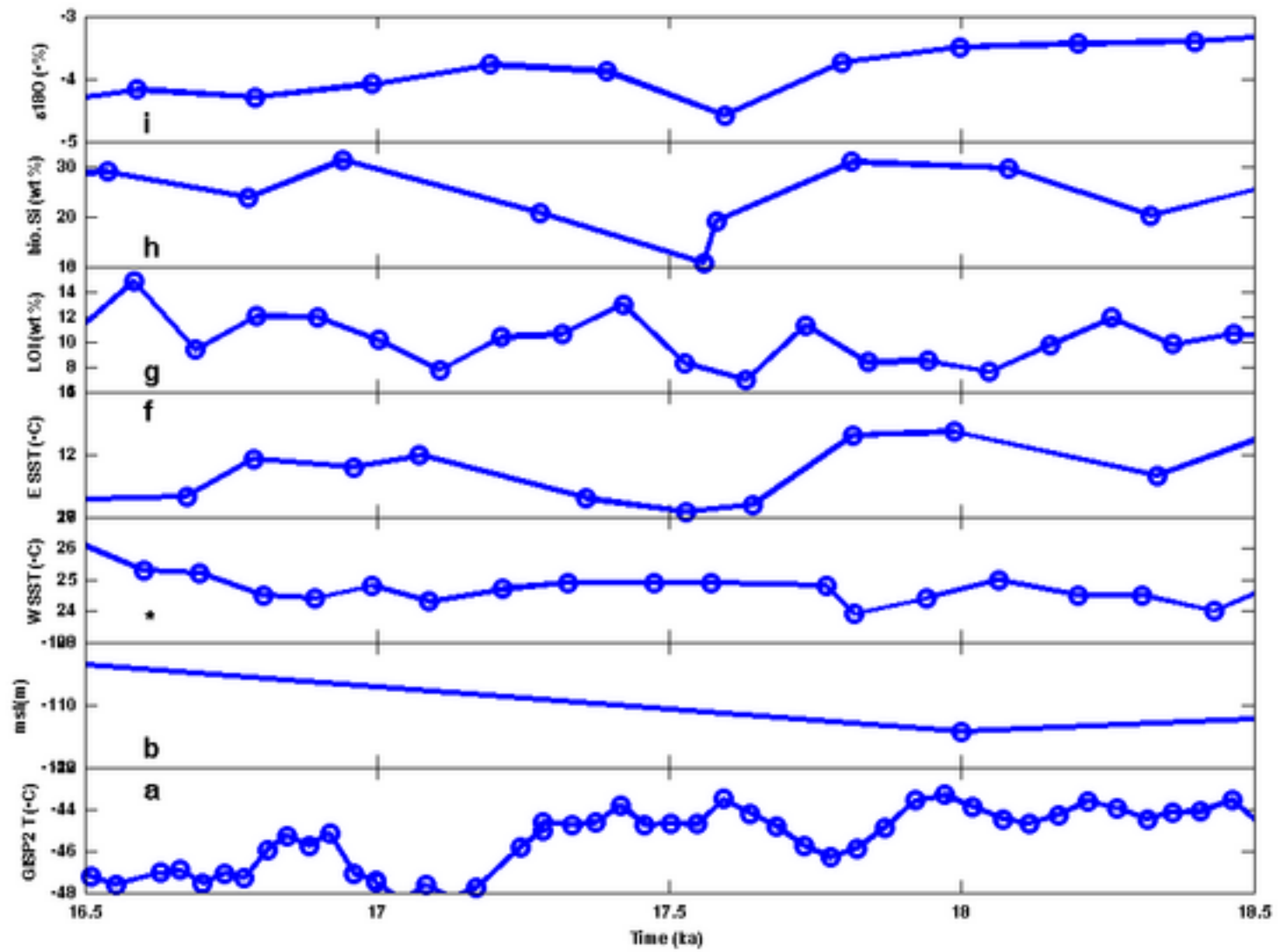


Figure 11

[Click here to download high resolution image](#)

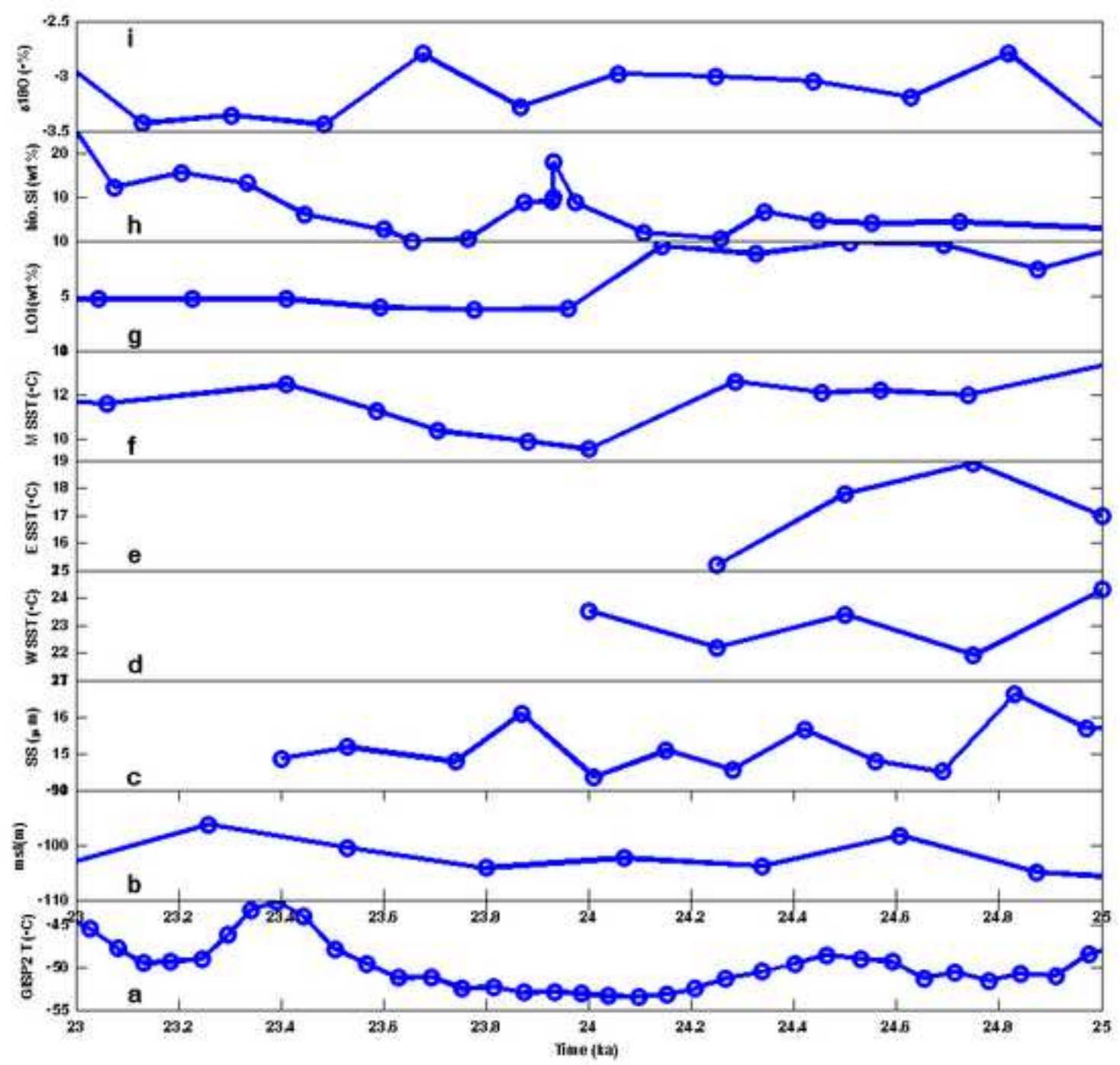


Figure 12  
[Click here to download high resolution image](#)

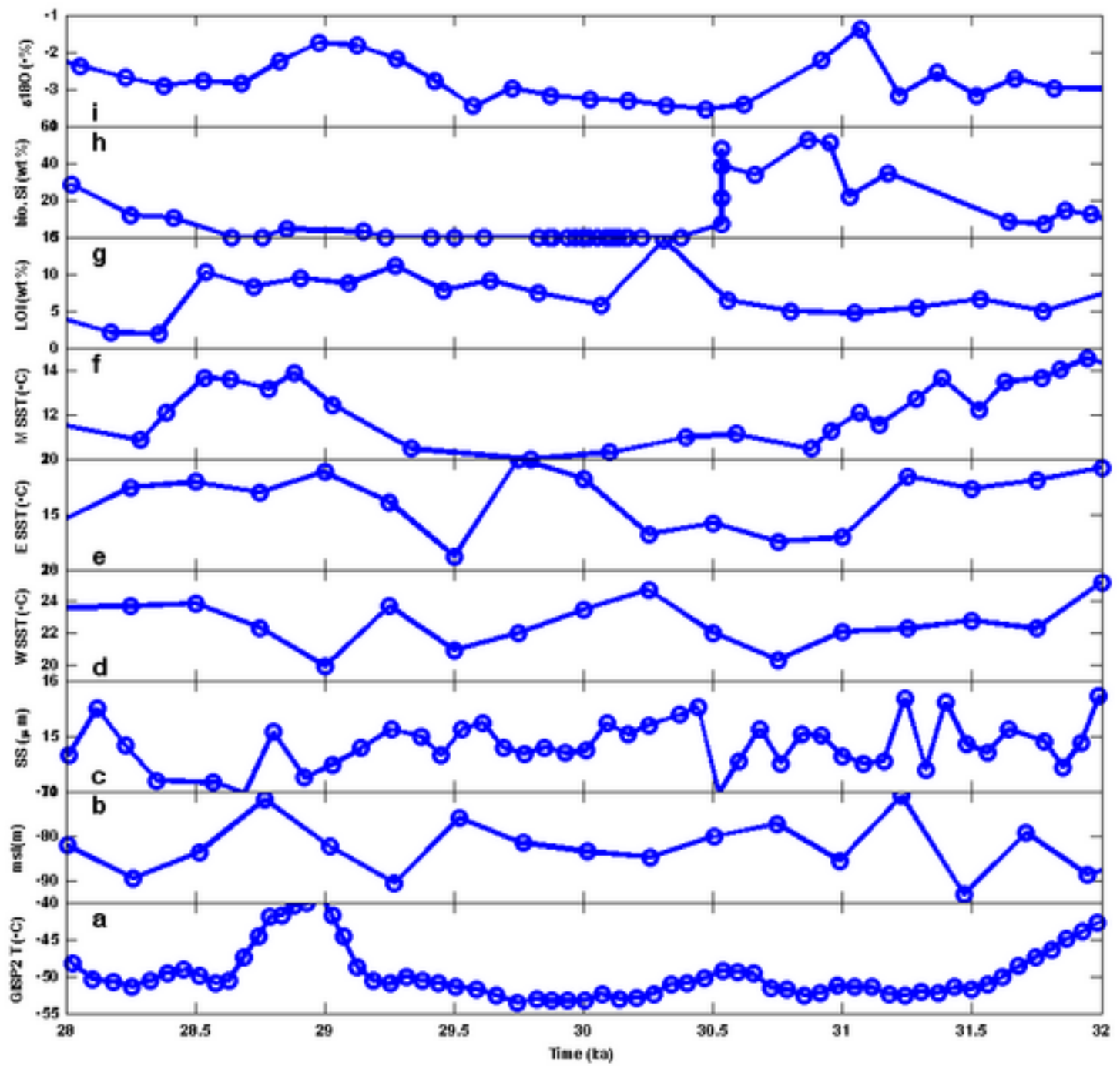


Figure 13

[Click here to download high resolution image](#)

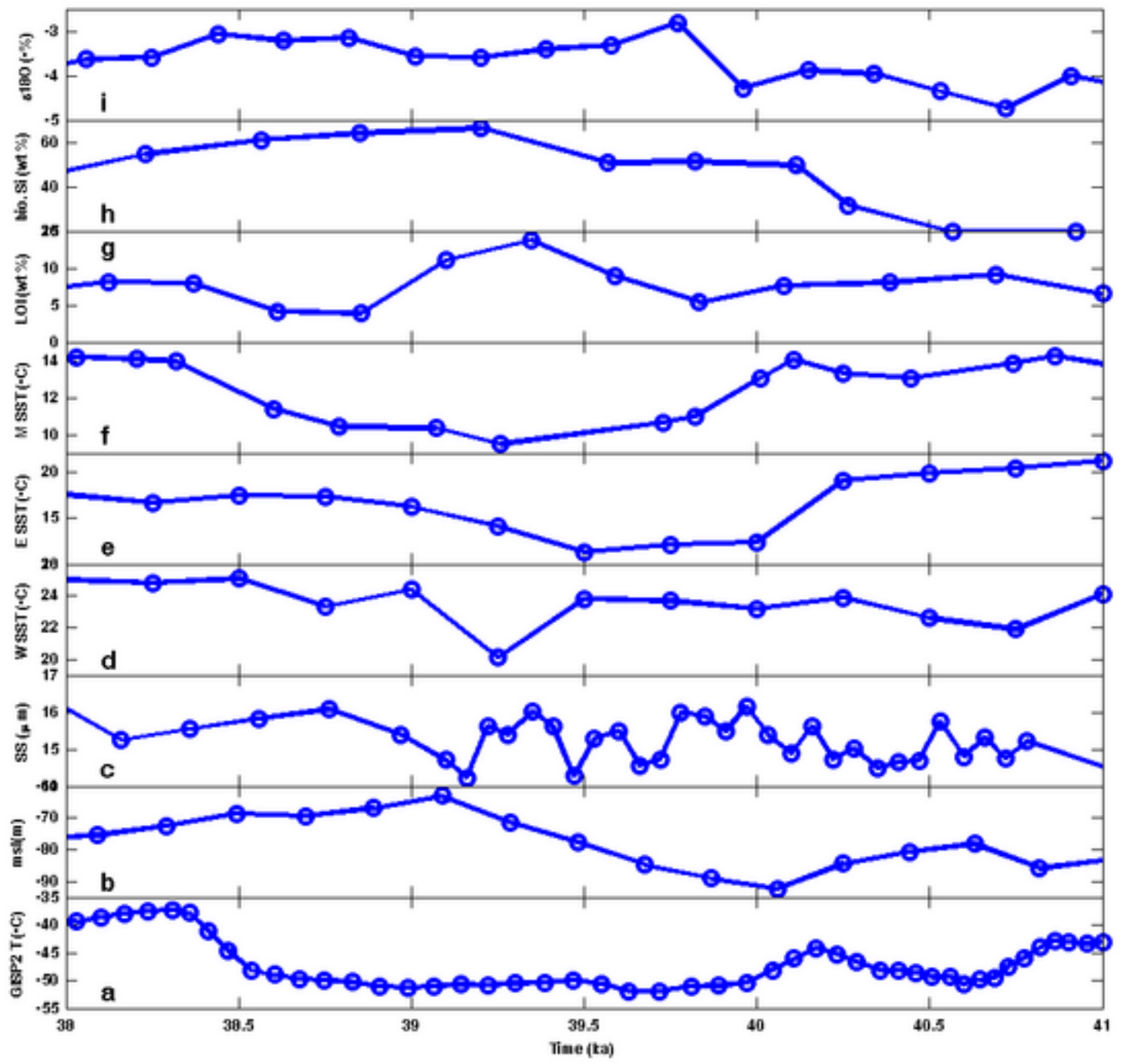




Figure 14

[Click here to download high resolution image](#)

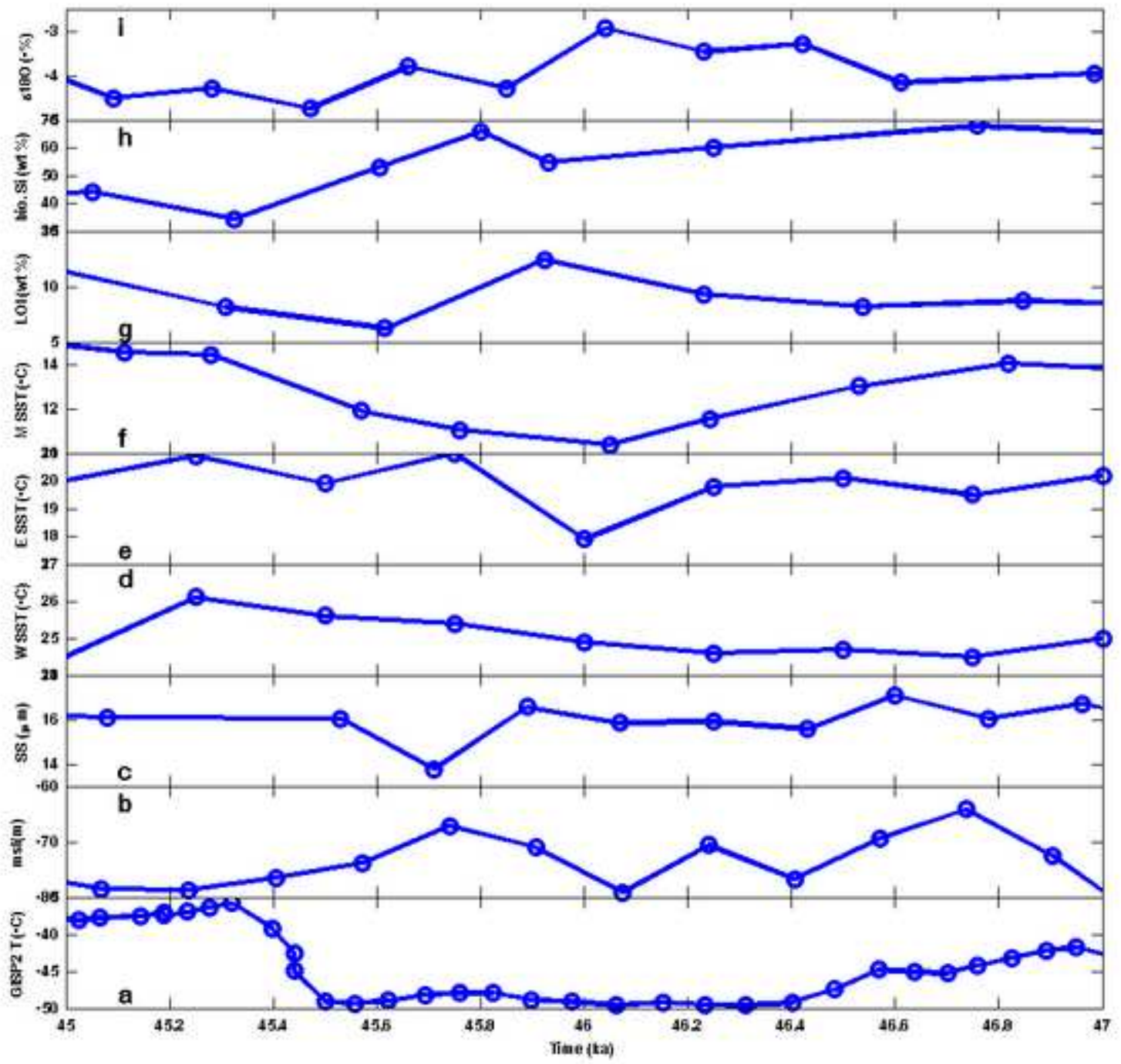


Figure 15

[Click here to download high resolution image](#)

